九州大学学術情報リポジトリ
Kyushu University Institutional Repository

# YAP signaling induces PIEZO1 expression to promote oral squamous cell carcinoma cell proliferation

Hasegawa, Kana
Laboratory of Oral Pathology, Division of Maxillofacial Diagnostic and Surgical Sciences, Faculty of Dental Science, Kyushu University

Fujii, Shinsuke
Laboratory of Oral Pathology, Division of Maxillofacial Diagnostic and Surgical Sciences, Faculty of Dental Science, Kyushu University

Matsumoto, Shinji
Department of Molecular Biology and Biochemistry, Graduate School of Medicine, Osaka University

田尻, 祐大
Laboratory of Oral Pathology, Division of Maxillofacial Diagnostic and Surgical Sciences, Faculty of Dental Science, Kyushu University

他

https://hdl.handle.net/2324/4481560

出版情報：Journal of Pathology. 253 (1), pp.80-93, 2021-01. Wiley
バージョン：
権利関係：

KYUSHU UNIVERSITY

# YAP signaling induces PIEZO1 expression to promote oral squamous cell carcinoma cell proliferation

**A short running title:** YAP signaling induces PIEZO1 expression to promote OSCC cell growth

Kana Hasegawa[1], Shinsuke Fujii[1*], Shinji Matsumoto[2], Yudai Tajiri[1,3], Akira Kikuchi[2] and Tamotsu Kiyoshima[1]

[1]Laboratory of Oral Pathology, Division of Maxillofacial Diagnostic and Surgical Sciences, Faculty of Dental Science, Kyushu University, 3-1-1 Maidashi, Higashi-ku, Fukuoka 812-8582, Japan

[2]Department of Molecular Biology and Biochemistry, Graduate School of Medicine, Osaka University, 2-2 Yamadaoka, Suita 565-0871, Japan

[3]Department of Dentistry and Oral Surgery, Clinical Research Institute, National Hospital Organization Kyushu Medical Center, 1-8-1 Jigyohama, Chuo-ku, Fukuoka 810-8563, Japan

[*]Corresponding author. Laboratory of Oral Pathology, Division of Maxillofacial Diagnostic and Surgical Sciences, Faculty of Dental Science, Kyushu University

3-1-1 Maidashi, Higashi-ku, Fukuoka 812-8582, Japan

Phone: +81-92-642-6328; Fax: +81-92-642-6329

E-mail: sfujii@dent.kyushu-u.ac.jp

For Peer Review

Conflict of interest statements: No conflicts of interests were declared.

A word count: 3,998

DNA microarray analysis was carried out in the current study, and the raw data reported in this study was deposited in NCBI GEO under accession number (GSE150044).

For Peer Review

**Abstract**

Most cancer cells are exposed to extracellular environments, such as an increase in extracellular matrix (ECM) stiffness with genetic transformation of cancer cells and soluble signals consisting of growth factors and cytokines. It is therefore conceivable that changes in the tumorous extracellular environments would affect tumor cell behavior. The Hippo pathway reportedly responds to the extracellular environment and regulates the nuclear localization of the transcription co-activator, yes-associated protein (YAP)/transcriptional co-activator with PDZ-binding motif (TAZ). Inactivation of the Hippo pathway with nuclear translocation of YAP/TAZ leads to stimulate cell proliferation. Its pathway also regulates gene expression, but the precise molecule meditating the cell-proliferating effect of YAP signaling on oral squamous cell carcinoma (OSCC) is unclear. First, we examined the effects of YAP signaling on OSCC tumorigenesis. Loss-of-function experiments using siRNA or an inhibitor, and immunohistochemical analyses of tissue specimens obtained from OSCC patients demonstrated that YAP signaling was involved in OSCC cell proliferation. Second, we identified Piezo-type mechanosensitive ion channel component 1 (PIEZO1), a $Ca^{2+}$ channel, as a transcriptional target of YAP signaling and showed that an elevated PIEZO1 expression was required for PIEZO1 agonist-dependent $Ca^{2+}$ entry and cell proliferation in OSCC cells. Furthermore, experiments using three-dimensional culture and suspension culture revealed that PIEZO1, the expression of which is regulated by YAP signaling, was involved in OSCC cellular growth. Finally, YAP overexpression in the nucleus and/or cytoplasm was immunohistochemically detected in tumor lesions with high

For Peer Review

frequent expression of both PIEZO1 and Ki-67 but not in non-tumor regions of OSCC specimens. These results suggest that the YAP/PIEZO1 axis promotes OSCC cell growth.

Key words: OSCC, YAP, PIEZO1, Proliferation, Three-dimensional culture, Suspension culture

For Peer Review

## Introduction

Oral squamous cell carcinoma (OSCC) is the 11th-most common cancer in the world [1], with over 300,000 new cases and 145,000 deaths every year [2]. The 5-year survival rate of OSCC patients is approximately 50% [3]. Although treatments for OSCC, including surgical resection, radiotherapy and chemotherapy, have been improving, the rate of recurrence is 20%-40%, resulting in a reduced survival rate [4,5]. Therefore, a novel cancer therapy based on the molecular mechanisms underlying OSCC tumorigenesis is awaited.

Tumor cells are exposed to the extracellular environments, such as ECM and soluble signals consisting of growth factors and cytokines [6]. Clinically, matrix stiffening is a prominent hallmark of the tumor microenvironment. In OSCC, stiffness is an important clinical feature. Recent studies showed novel mechanotrasduction mechanisms, in which an increase in tumorous ECM stiffness drove tumor progression through the activation of intracellular signaling, such as β1 integrin-FAK signaling and RHOA-AKT-p300 signaling in breast cancer and liver cancer, respectively [7,8]. We also demonstrated that transient receptor potential vanilloid 4 (TRPV4), a $Ca^{2+}$ channel, responds to the extracellular stiffness, which in turn promoting OSCC cell proliferation through CaMKII-AKT activation [9]. These reports indicate that tumorous extracellular environments could affect tumor cell behavior through several mechanotrasduction machineries.

The Hippo pathway responds to the extracellular environments and stimulates cell proliferation, through regulating the nuclear localization of major downstream effectors, yes-associated protein (YAP)/transcriptional co-activator with PDZ-binding motif (TAZ),



http://mc.manuscriptcentral.com/jpath

For Peer Review

resulting in the induction of transcriptional target expression [10-13]. Its pathway has been involved in tumorigenesis in OSCC and hepatocellular carcinoma and is associated with the poor prognosis in breast cancer, ovarian cancer and hepatocellular carcinoma [14-17], but transcriptional targets that mediate the function of the Hippo pathway are not well understood.

Piezo-type mechanosensitive ion channel component (PIEZO) channels, including PIEZO1 and PIEZO2, were identified as mechanically activated ion channels [18]. PIEZO1 is reportedly associated with epithelial cellular division, neural cell differentiation and vasculature development by sensing mechanical stress, such as cell density, substrate stiffness and shear stress [19-21]. Although the effects of PIEZO1 on tumorigenesis have been demonstrated [22-25], its function and expression mechanism in OSCC tumorigenesis remain unclear. Recent reports showed that the depletion of PIEZO1 expression induced nuclear exclusion of YAP in human neural stem cells and zebrafish outflow tract valve development [20,26], suggesting that PIEZO1 could act as an upstream of YAP. But, the hierarchical relationship between YAP and PIEZO1 is unclear in OSCC. We conducted a study to clarify their relationship in OSCC and elucidate the function of PIEZO1 to control OSCC cellular growth using cell lines and pathological specimens.

For Peer Review

## Materials and methods

### Cell lines and reagents

Human OSCC cell lines HSC-4, HSC-3, HSC-2, SAS (Japanese Cancer Research Resources Bank), MISK81-5 and sMISK [27], human gastric cancer cell line MKN-45 (Japanese Cancer Research Resources Bank) and human lung adenocarcinoma cell line A549 [28] were used in this study. HSC-4, HSC-3, HSC-2, MISK81-5 and sMISK were maintained in α-MEM (Invitrogen, Carlsbad, CA, USA), SAS and A549 were maintained in D-MEM (Invitrogen), and MKN-45 was maintained in RPMI-1640 (Invitrogen). These culture media were supplemented with 10% FBS (Invitrogen), and contained 100 IU/ml penicillin and 100 mg/ml streptomycin (Invitrogen). All these cell lines were incubated at 37°C in a 5% $CO_2$ atmosphere. See supplementary Materials and methods for further details.

### Knockdown of protein expression by siRNA and quantitative RT-PCR

The effects of protein knockdown by siRNA were analyzed as previously described [29]. Briefly, siRNAs (final conc. 20 nM) were transfected into OSCC cells using Lipofectamine RNAiMAX (Invitrogen). Target sequences are listed in supplementary material (Table S1). The transfected cells were then used for experiments conducted at 48 h post-transfection.

Quantitative RT-PCR was performed as described previously [29]. Primers are listed in supplementary material (Table S2).

For Peer Review

**Plasmid construction and infection using lentivirus harboring a cDNA or shRNA**

The YAP$^{5SA}$ plasmid, CSII-CMV-MCS-IRES2-Bsd/FLAG-YAP$^{5SA}$, was used [12]. To construct a lentiviral vector harboring shRNA, a DNA fragment containing the H1 promoter and shRNA was cloned into CS-RfA-EVBsd, which was kindly provided by Dr. H. Miyoshi (RIKEN BioResource Center, Ibaraki, Japan) [30], using Gateway technology (Invitrogen). Target sequence is #1 5'-AGAAGAAGATCGTCAAGTA-3' or #2 5'- ACCAACCTCATCAGCGACT-3'. The vectors were then transfected along with the packaging vectors, pCAG-HIV-gp and pCMV-VSV-G-RSV-Rev, into X293T cells using the Lipofectamine LTX reagent (Invitrogen) to generate lentiviruses [28]. See supplementary Materials and methods for further details.

**Three-dimensional culture and suspension culture**

3D culture was prepared using collagen gel culture kit Tri-D (Nippi, Inc.) or Matrigel (BD Biosciences, San Jose, CA, USA) according to the manufacturer's protocol. Briefly, bottom collagen gel (1 mg/ml) was poured into the dishes and incubated for polymerization for 30 min at 37°C. Then, cells mixed with 1 mg/ml collagen gel were layered onto the bottom gel. Culture medium was added on top, and then cells cultured in 3D culture were incubated at 37°C. 40 µl of Matrigel was mounted on a round coverslip and incubated for 30 min at 37°C to solidify the gel, and cells ($4 \times 10^4$ cells) suspended in 1 ml of growth medium containing 2% Matrigel (v/v) were incubated for 96 h [9,31].

For Peer Review

In suspension culture, the cells ($2 \times 10^5$ cells) were cultured with growth medium in low-attachment 1.5 ml tube (Sumitomo Bakelite Co., Ltd, Tokyo, Japan) for 24 h.

**Cell proliferation assay**

To examine proliferative capabilities in 2D culture, 3D culture or suspension culture, CyQUANT NF assay (Invitrogen) was performed according to the manufacturer's protocol. Then, the fluorescence intensity was measured using FlexStation 3 microplate reader (Molecular Devices, Tokyo, Japan) at 485 nm excitation/530 nm emission.

**ChIP assay**

ChIP assay was performed as described previously [32]. HSC-4 cells ($1 \times 10^7$) were cross-linked with 1% (v/v) formaldehyde for 20 min at room temperature. The cells were lysed and sonicated to shear DNA to a size range between 200 and 1000 bp. Sheared chromatin samples were incubated for 4 h at 4°C with 10 μg of antibodies. Immunocomplexes were absorbed with salmon sperm DNA/protein A-agarose beads. See supplementary Materials and methods for further details.

**Intracellular calcium measurement**

Intracellular calcium measurement was performed as described previously [9]. See supplementary Materials and methods for further details.

**Immunocytochemistry**

For Peer Review

Immunocytochemistry was carried out as previously described [33]. See supplementary Materials and methods for further details.

**Patients and immunohistochemistry**

A total of 45 patients with ages ranging from 42 to 90 years (median, 70 years) with primary OSCC diagnosed for treatment at the Department of Oral and Maxillofacial Surgery, Kyushu University Hospital, Japan, from March 2011 to February 2020 were examined in this study. The protocol for this study was approved by the ethical review board of the Local Ethical Committee of Kyushu University, Japan (#30-235). Following the initial biopsy, all specimens were fixed in 10% (v/v) formalin and embedded in paraffin blocks. Subsequently, the paraffin-embedded specimens were sliced into 4-μm-thick sections, stained with hematoxylin-eosin (HE), and examined by three experienced pathologists to confirm the diagnoses and the histological grades. The histological grade in the OSCC was assessed according to the WHO classification [34]. The tumor extent and the clinical stages were evaluated according to the TNM classification established by the American Joint Committee on Cancer and the International Union Against Cancer (UICC) [35]. The medical records were reviewed to collect information on the clinical characteristics. The clinicopathological data of the patients with OSCC are presented in Table 1 and 2. Immunohistochemical staining was performed as previously described [9]. See supplementary Materials and methods for further details.

**Microarray analysis**





For Peer Review

Microarray analyses were performed using HSC-4 cells cultured in 2D culture or suspension culture as previously described [33]. The raw data reported in this study was deposited in NCBI GEO under accession number (GSE150044). Gene Ontology (GO) analysis was performed using DAVID database (http://david.abcc.ncifcrf.gov/). See supplementary Materials and methods for further details.

**Analysis of TCGA head and neck cancer dataset**

*PIEZO1*, *PIEZO2*, *amphiregulin* (*AREG*) and *cyclin dependent kinase 6* (*CDK6*) gene expression data for 518 head and neck tumor lesions and 44 non-tumor regions were obtained from The Cancer Genome Atlas (TCGA) web site (http://tcga-data.nci.nih.gov/tcga/tcgaHome2.jsp).

**Statistical analysis**

Significant differences were determined using Fisher's exact test for Table 1 and 2. For other experiments, significant differences were determined using Student's t test and one-way ANOVA with turkey. *P* value of $< 0.05$ or 0.01 was considered statistically significant.

For Peer Review

## Results

### Proliferative capabilities of oral squamous cell carcinoma cells in three-dimensional and suspension culture

Inactivation of the Hippo pathway regulates YAP/TAZ nuclear translocation, thereby inducing transcriptional targets and promoting cell proliferation [10-17]. YAP/TAZ siRNA and the treatment with simvastatin, a YAP inhibitor [36,37], reduced not only the mRNA levels of *ankyrin repeat domain1* (*ANKRD1*) and *cellular communication network factor 1* (*CCN1*; also known as *CYR61*), which are transcriptional targets of YAP/TAZ, but also 2-dimentional (2D) proliferation of HSC-4 cells (supplementary material, Figure S1A). These loss-of-function experiments indicated that YAP/TAZ signaling was involved in HSC-4 cell proliferation. Next, we conducted to set up the cell culture system, which is capable of analyzing the relationship between YAP/TAZ signaling and its transcriptional targets.

Our recent study showed that HSC-4 cells respond to extracellular environments, such as 3D culture with Matrigel and 2D plastic dish culture, and exhibited lower proliferation capabilities in 3D culture than in 2D culture [9]. Consistently, the cellular growth in 3D culture with collagen gel was also suppressed compared with 2D culture in HSC-4 and HSC-3 cells (Figure 1A), indicating that extracellular conditions do indeed affect OSCC cellular proliferation capabilities, regardless of the matrix. Proliferative capabilities in suspension culture were extremely lower than 2D or 3D culture (Figure 1A). As YAP signaling could be inactivated in suspension culture [12], we carried out a microarray analysis using HSC-4 cells cultured in 2D and suspension culture. Expectedly, GO

For Peer Review

analysis showed enrichment for previously reported the YAP/TAZ function, such as DNA replication, mitotic nuclear division, DNA replication initiation, regulation of cell cycle, cell proliferation, DNA repair, cell cycle and positive regulation of cell migration (Figure 1B and supplementary material, Table S3). Indeed, transcriptional targets of YAP/TAZ, such as *AREG*, *aurora kinase B* (*AURKB*), *cyclin D1*(*CCND1*), *CDK6*, *E2F transcription factor 1* (*E2F1*), *forkhead box M1*(*FOXM1*), *kinesin family member 23* (*KIF23*) and *minichromosome maintenance complex component 7* (*MCM7*) [38-44] were listed as a down-regulated gene in suspension culture (supplementary material, Table S4). These data suggested that suspension culture could be useful to identify transcriptional targets of YAP/TAZ signaling. In suspension culture, YAP/TAZ expression was reduced in a time-dependent manner (Figure1C). Similarly, the mRNA levels of *ANKRD* and *CYR61* were reduced in OSCC cells in suspension culture compared with 2D culture (Figure 1D and supplementary material, Figure S1B). In addition, siRNA treatment for large tumor suppressor 2 (LATS2), which phosphorylates YAP/TAZ on serine residues [10], reversed the suspension culture-dependent decrease of *ANKRD1*, *CYR61, AURKB* and *FOXM1* expression (Figure 1E and supplementary material, Figure S1C and S1D). These results indicate that YAP/TAZ signaling may be inactivated in the suspension culture, thereby suppressing cell proliferation in OSCC cells.

**PIEZO1 is a transcriptional target of YAP signaling in oral squamous cell carcinoma cells**

PIEZO channels, including PIEZO1 and PIEZO2, were identified as mechanically





For Peer Review

activated ion channels [18]. The Cancer Genome Atlas (TCGA) dataset showed that *PIEZO1* and *PIEZO2* mRNA were elevated in tumor lesions compared with in non-tumor regions, but *PIEZO2* mRNA expression levels were lower than that of *PIEZO1* in head and neck region (supplementary material, Figure S2A). Although PIEZO1 has been demonstrated both positive [22,23] and negative [24,25] effects on tumorigenesis, its function and expression mechanism in OSCC tumorigenesis remain unclear. Therefore, the function of PIEZO1 in OSCC tumorigenesis was investigated in the current study. Previous report showed YAP activation in OSCC tumor lesion [37]. Consistently, the expression of *AREG* or *CDK6* was elevated in tumor lesions. Since a significant correlation between *PIEZO1* and *AREG* or *CDK6* was observed (supplementary material, Figure S2A), it is possible that *PIEZO1* expression is correlated with YAP signaling. It has been reported that PIEZO1 could act as an upstream of YAP in the developmental stages [20,26]. Therefore, we conducted to clarify the relationship between YAP/TAZ signaling and PIEZO1 in OSCC cells in the subsequent experiments.

PIEZO1 expression was decreased in 3D culture compared with 2D culture in HSC-4 cells (Figure 2A), and was also reduced in suspension culture (Figure 2B and supplementary material, Figure S2B). Importantly, knockdown of LATS2 rescued the suspension culture-dependent reduction of the expression of *PIEZO1* in HSC-4 cells (Figure 2C), suggesting that YAP/TAZ signaling may act as an upstream of PIEZO1. In addition, two different YAP/TAZ siRNAs reduced *PIEZO1* expression in HSC-4 and HSC-3 cells (Figure 2D and supplementary material, Figure S2C). To elucidate the function of YAP, HSC-4 and HSC-3 cells expressing mock or an active YAP mutant

For Peer Review

YAP$^{5SA}$, in which five possible phosphorylation serine residues are changed to alanine [12,45], were generated by lentiviral transduction. In YAP$^{5SA}$-expressing OSCC cells, the expression of PIEZO1, as well as *ANKRD1* and *CYR61*, was elevated compared with mock-expressing cells, indicating that YAP activation induces PIEZO1 expression (Figure 2E and supplementary material, Figure S2C and S2D). We conducted to find the putative binding sites of TEA domain transcription factors 4 (TEAD4), which is a major transcription factor in the Hippo pathway regulating the expression of transcriptional targets associated with YAP/TAZ [46], using Cistrome Data Browser database (http://cistrome.org/db/#/) in human *PIEZO1* gene. The database showed that ChIP-seq peaks of TEAD4 and active histone modifications, such as H3K27ac and H3K9ac, were hardly detected in the region upstream from the TSS of *PIEZO1* gene. In contrast, three ChIP-seq peaks of TEAD1 or TEAD4, which are commonly detected in multiple cell lines and contain putative binding sites of four TEAD genes (data not shown), were found within the *PIEZO1* gene body. Site 1 is located within exon 1, and site 2 and site 3 were located between exons 1 and 2. In addition, these sites overlapped the peaks of H3K27ac and H3K9ac, and exhibited high enhancer activity region using epilogos database (https://epilogos.altius.org) (supplementary material, Figure S2E). ChIP assay revealed that TEAD4 indeed bound to *PIEZO*1 gene more dominantly through sites 2 and 3, as well as to promoter region of *ANKRD1* as a positive control [47], than in site 1 (Figure 2F and supplementary material, Figure S2E). Furthermore, YAP$^{5SA}$ also formed a complex with sites 2 and 3 (Figure 2F). Previous report showed that YAP activity is mediated via TEADs binding to not only promoters but also enhancers of the

For Peer Review

transcriptional targets [47]. Therefore, the current TEAD4 binding sites could be involved in PIEZO1 expression mechanism. These results suggest that PIEZO1 is a possible transcriptional target of YAP signaling.

**PIEZO1 expression is involved in agonist-induced ERK1/2 and p38 MAPK activation**

*PIEZO1* or *PIEZO2* expression in cancer cell lines was analyzed using Cancer Cell Line Encyclopedia (https://portals.broadinstitute.org/ccle) dataset, which was viewed by cBioportal (https://www.cbioportal.org). In HSC-2, HSC-3 and HSC-4 cells, *PIEZO1* was expressed to the similar levels to other cancer cells, while *PIEZO2* expression was little expressed in many cancer cells (supplementary material, Figure S3A). We also measured *PIEZO1* expression in six human OSCC cell lines and a control gastric cancer cell line. HSC-4 and HSC-3 highly expressed *PIEZO1* (Figure 3A), while *PIEZO2* mRNA level was low in OSCC cell lines, compared with A549 cells (supplementary material, Figure S3B). Treatment with Yoda1, a specific PIEZO1 agonist [48,49], increased the intracellular $Ca^{2+}$ influx in a dose-dependent manner in HSC-4 cells (Figure 3B and supplementary material, Figure S3C). Two different siRNAs knocked down PIEZO1 mRNA and protein, but not *PIEZO2* mRNA expression (Figure 3C and supplementary material, Figure S3D). Importantly, PIEZO1 knockdown did not change the mRNA levels of YAP transcriptional targets, such as *ANKRD1* and *CYR61*, and YAP/TAZ nuclear localization, indicating that YAP signaling would not be regulated by PIEZO1 in OSCC cells (supplementary material, Figure S3D). Knockdown of PIEZO1

For Peer Review

suppressed the Yoda1-dependent $Ca^{2+}$ influx (Figure 3D and supplementary material, Figure S3E). Since Yoda1 treatment stimulated ERK1/2 and p38 MAPK activation in human bone marrow-derived mesenchymal stem cells [50], the effect of PIEZO1 on its activation was examined in HSC-4 cells. PIEZO1 knockdown reduced Yoda1-induced ERK1/2 and p38 MAPK phosphorylation, but did not affect the AKT phosphorylation (Figure 3E). Supporting our results, previous report revealed that gain-of-function mutations in PIEZO1 increased $Ca^{2+}$ concentrations with ERK1/2 activation, indicating that the expression of PIEZO1 channel activates intracellular signaling [51]. These results suggest that PIEZO1 may function as an ion channel and its expression is involved in agonist-dependent ERK1/2 and p38 MAPK activation in OSCC cells.

**PIEZO1 expression is required for cell proliferation in oral squamous cell carcinoma cells**

As ERK1/2 and p38 MAPK activation is involved in cell proliferation [52,53], the effect of PIEZO1 on cell proliferation was examined in OSCC cells. Knockdown of PIEZO1 decreased the ratio of Ki-67-positive or PCNA-positive cells and cell proliferation capability in HSC-4 cells (Figure 4A and 4B, and supplementary material, Figure S4A), but did not increase the number of cleaved caspase-3-positive cells (supplementary material, Figure S4B). GsMTx-4, a mechanosensitive and stretch-activated ion channel inhibitor and also functions as an inhibitor of PIEZO1 [20,51], decreased cell proliferation (Figure 4C). To further clarify the function of PIEZO1, we generated HSC-4 cells stably expressing PIEZO1 #1 or #2 shRNA (Figure 4D). Based on the above results using

For Peer Review

siRNAs, target sequences of PIEZO1 #1 and #2 shRNAs were designed to be identical to those of PIEZO1 #1 and #2 siRNAs, respectively. In these cells, Yoda1-dependent $Ca^{2+}$ influx was suppressed, which was consistent with our experiments using siRNAs (Figures 3D and 4E, and supplementary material, Figure S4C). In 3D culture, LATS2 knockdown or $YAP^{5SA}$ expression increased the ratio of Ki-67- or PCNA-positive cells in control cells (Figure 4F and 4G and supplementary material, Figure S4D). Importantly, in HSC-4 cells expressing PIEZO1 #1 or #2 shRNA, LATS2 knockdown or $YAP^{5SA}$ expression did not change the ratio of Ki-67- or PCNA-positive cells and induced the expression of *ANKRD1*, but not *PIEZO1* (Figure 4F and 4G and supplementary material, Figure S4E). These results suggest that YAP signaling promotes cell proliferation through inducing PIEZO1 expression in 3D-cultured OSCC cells.

**PIEZO1 and YAP are expressed in human oral squamous cell carcinoma tissues**

Immunohistochemical analyses were performed to examine PIEZO1 and YAP expression in human OSCC specimens. PIEZO1 expression was detected in 45/45 (100%) tumor lesions and 25/31 (80.6%) non-tumor regions (Figure 5A and supplementary material, Figure S5). Based on the intensity of the PIEZO1-positive signal, the samples were divided into three groups: negative, weak and strong (Figure 5A). PIEZO1 was strongly expressed in the cellular cytoplasm in 23/45 (51.1%) tumor lesions, while a strong expression was noted in 2/31 (6.5%) non-tumor regions, showing a significant difference ($p<0.0001$; Fisher's exact test) (Figure 5A).

Based on the YAP expression and localization, specimens were divided into three





For Peer Review

groups: negative, nucleus/cytoplasm and nucleus (supplementary material, Figure S6A). When YAP was expressed in nucleus/cytoplasm or nucleus, the results were defined as a YAP-positive case, in which the ratio of YAP-positive cells was more than 30% in a tumor lesion or a non-tumor region. YAP-positive cases were 43/45 (95.6%) in tumor lesions, while those were 10/31 (32.3%) in non-tumor regions (supplementary material, Figure S6B), showing a significant difference ($p<0.0001$; Fisher's exact test). Notably, YAP was hardly detected in nucleus in non-tumor regions. Mice with tongue-specific deletion of MOB kinase activator 1A/B developed tongue carcinoma through endogenous YAP1 hyperactivation, in which YAP1 was localized in nucleus at high frequencies [37]. Therefore, we speculated that YAP might be hyperactivated in tumor lesions of our OSCC specimens. As expected, the YAP-positive expression was frequently detected in tumor lesions with Ki-67 expression but not in non-tumor regions (Figure 5B and supplementary material, Figure S6C), suggesting that hyperactivated YAP might promote cancer cell proliferation. Significant correlations with the PIEZO1 intensity or the YAP expression and localization were not shown for the clinical T (tumor size) stage, histological grade and lymph node metastasis (Table 1 and 2). It is noteworthy that YAP-positive cases with a strong PIEZO1 expression in tumor lesions were more frequent, but not significantly, than in non-tumor regions in consecutive sections (Figure 5B and supplementary material, Figure S7). Taken together, these results suggest that YAP, which might be hyperactivated in tumor lesion, likely induces PIEZO1 expression, resulting in enhanced OSCC cell proliferation.

For Peer Review

## Discussion

It is generally accepted that the changes in the tumorous extracellular environments, including ECM stiffness and exposure to soluble signals, affect tumor cell behavior [6]. We aimed to identify a molecule, which is activated by extracellular environments, to regulate OSCC tumorigenesis. In the current suspension culture and 3D culture, OSCC cell proliferation capabilities were reduced. Subsequently, we identified PIEZO1 as a transcriptional target of YAP signaling and showed that an elevated PIEZO1 expression was required for cell proliferation of OSCC cells.

To our knowledge, this is the first report to suggest that PIEZO1 might function as an oncogene-related molecule in OSCC. Similar to our immunohistochemical data, PIEZO1-positive signals were detected in the cytoplasm of human prostate carcinoma tissue [23]. In Madin-Darby canine kidney normal epithelial cells, PIEZO1 developed into large cytoplasmic aggregates in the crowded regions with increased cell density [19]. Considering these results, the cytoplasmic localization of PIEZO1 in tumor lesions would correlate with its function, but underlying mechanism is not clear. Cryo-electron microscopy and high-speed atomic force microscopy showed that PIEZO1 structural deformation gates its channel in response to mechanical stress [54], thereby inducing $Ca^{2+}$ influx [55]. Therefore, the effects of PIEZO1 on OSCC tumorigenesis might depend on PIEZO1 expression level.

In the present study, suspension culture was used to elucidate the hierarchical relationship between YAP and PIEZO1. At present, we do not know why PIEZO1 was not suggested as a down-regulated gene in the microarray data (supplementary material,





For Peer Review

Table S4).

Recently, it has been reported that PIEZO1 could act as an upstream of YAP in the developmental stages, such as human neural stem cell differentiation and zebrafish heart development [20,26]. In this study, PIEZO1 knockdown did not affect the expression of YAP transcriptional targets and YAP/TAZ nuclear localization. In addition, gain-of-function experiments and ChIP data demonstrated that YAP signaling promotes PIEZO1 expression in OSCC cells. Although the hierarchical relationship between YAP signaling and PIEZO1 may depend on cell context, it is noteworthy that these molecules could be a common mechanotransduction mechanism between organ formation by stem cells and tumor formation by cancer cells.

The current immunohistochemical data demonstrated YAP localization in nucleus and/or cytoplasm in tumor lesions with an increased Ki-67-positive signal, suggesting that YAP signaling might be activated with enhanced OSCC cellular growth. But underlying mechanism to activate YAP signaling is unclear. In non-tumor regions, we also confirmed a low frequency of YAP-positive expression in nucleus/cytoplasm with a decreased Ki-67-positive signal (see supplementary material, Figure S6C), but its precise function in the regions remains unclear. As the Hippo pathway regulates cell differentiation as well as cell proliferation [45], cancer therapy targeting for components of the Hippo pathway might cause side effects in the non-tumor region, at least in OSCC. If the transcriptional targets mediating the Hippo pathway in regulating cellular growth may function in tumor lesion specifically, its gene could be a molecular target for novel cancer therapy.

For Peer Review

Some genetic mutations of cancer-related genes, which are responsible for tumorigenesis and might be molecular targets of anti-tumor therapy for OSCC, have been reported [56]. Recent report also demonstrated that the resistance to phosphoinositide-3-kinase (PI3K)-α inhibitors for head and neck SCC bearing PIK3 catalytic subunit alpha (PIK3CA) mutations and amplification [57], indicating that the therapeutic options for patients with head and neck SCC are limited. Another molecular mechanism could be involved in OSCC tumorigenesis. We previously demonstrated that TRPV4, a $Ca^{2+}$ channel, enhances OSCC cell proliferation through CaMKII-AKT activation [9]. Given the present and previous findings, it is intriguing to speculate that $Ca^{2+}$ influx-dependent cellular growth through PIEZO1 or TRPV4 may be a potential target for anti-tumor therapy.

In summary, we found that YAP, which is activated in OSCC tumor lesion, promotes cancer cell proliferation. We also demonstrated that YAP signaling induces PIEZO1 expression to regulate OSCC cellular growth positively. Taken together, these results suggest that the YAP/PIEZO1 axis contributes to OSCC cell growth.

For Peer Review

**Acknowledgments**

The authors thank Drs. T. Harada, M. Nishio, A. Suzuki, I. Imajo and H. Wada for advices and searching clinical information in this research. The authors also thank the Research Support Center, Graduate School of Medical Sciences, Kyushu University. This work was supported by JSPS KAKENHI Grants to K. H. (2017-2018) (17K17103), (2019-2020) (19K18966), S. F. (2020-2022) (20K09906) and T. K. (2020-2022) (20K10096), and Takeda Science Foundation and The Shin-Nihon Foundation of Advanced Medical Research to S.F.

**Author contributions**

K. H. carried out experiments, analyzed data and co-wrote the manuscript. S. F. carried out experiments, conceived and wrote the manuscript. S. M. and A. K. performed ChIP experiments. Y. T. analyzed immunohistochemical data. T. K. carried out data interpretation and co-wrote the manuscript. All authors were involved in writing the paper and had final approval of the submitted and published versions.

For Peer Review

**Supporting Information**

**Supplementary figure legends**

**Figure S1.** The effect of YAP/TAZ signaling on OSCC cells.

**Figure S2.** YAP signaling regulates PIEZO1 expression in OSCC cells.

**Figure S3.** The effect of PIEZO1 on YAP/TAZ signaling.

**Figure S4.** PIEZO1 regulates cell proliferation of OSCC cells.

**Figure S5.** PIEZO1 is expressed in human oral squamous cell carcinoma tissues.

**Figure S6.** YAP is expressed in human oral squamous cell carcinoma tissues.

**Figure S7.** Co-expression of PIEZO1, YAP, Ki-67 and PCNA in human oral squamous cell carcinoma tissues.

**Table S1.** List of siRNA sequence used in this study.

**Table S2.** List of quantitative RT-PCR primer used in this study.

**Table S3.** Gene enrichment analysis in HSC-4 cells.

**Table S4.** List of gene from microarray analysis data of HSC-4 cells cultured in 2D culture and suspension culture.

For Peer Review

## References


1. Warnakulasuriya S. Global epidemiology of oral and oropharyngeal cancer. *Oral Oncol* 2009; **45**: 309-316.
2. Bray F, Ferlay J, Soerjomataram I, *et al.* Global cancer statistics 2018: GLOBOCAN estimates of incidence and mortality worldwide for 36 cancers in 185 countries. *CA Cancer J Clin* 2018; **68**: 394-424.
3. Bloebaum M, Poort L, Böckmann R, *et al.* Survival after curative surgical treatment for primary oral squamous cell carcinoma. *J Craniomaxillofac Surg* 2014; **42**: 1572-1576.
4. Anderson CR, Sisson K, Moncrieff M. A meta-analysis of margin size and local recurrence in oral squamous cell carcinoma. *Oral Oncol* 2015; **51**: 464-469.
5. Wang B, Zhang S, Yue K, *et al.* The recurrence and survival of oral squamous cell carcinoma: a report of 275 cases. *Chin J Cancer* 2013; **32**: 614-618.
6. Fares J, Fares MY, Khachfe HH, *et al*. Molecular principles of metastasis: a hallmark of cancer revisited. *Signal Transduct Target Ther* 2020; **5**: 28.
7. Levental KR, Yu H, Kass L, *et al.* Matrix crosslinking forces tumor progression by enhancing integrin signaling. *Cell* 2009; **139**: 891-906.
8. Dou C, Liu Z, Tu K, *et al.* P300 Acetyltransferase Mediates Stiffness-Induced Activation of Hepatic Stellate Cells Into Tumor-Promoting Myofibroblasts. *Gastroenterology* 2018; **154**: 2209-2221.
9. Fujii S, Tajiri Y, Hasegawa K, *et al.* The TRPV4-AKT axis promotes oral squamous cell carcinoma cell proliferation via CaMKII activation. *Lab Invest* 2020; **100**: 311-323.
10. Saucedo LJ, Edgar BA. Filling out the Hippo pathway. *Nat Rev Mol Cell Biol* 2007; **8**: 613-621.
11. Dupont S, Morsut L, Aragona M, *et al.* Role of YAP/TAZ in mechanotransduction. *Nature* 2011; **474**: 179-183.
12. Matsumoto S, Fujii S, Sato A, *et al.* A combination of Wnt and growth factor signaling induces Arl4c expression to form epithelial tubular structures. *EMBO J* 2014; **33**: 702-718.
13. Meng Z, Qiu Y, Lin KC, *et al.* RAP2 mediates mechanoresponses of the Hippo pathway. *Nature* 2018; **560**: 655-660.


For Peer Review

14. Hiemer SE, Zhang L, Kartha VK, *et al.* A YAP/TAZ-Regulated Molecular Signature Is Associated with Oral Squamous Cell Carcinoma. *Mol Cancer Res* 2015; **13**: 957-968.
15. Xu MZ, Yao TJ, Lee NP, *et al.* Yes-associated protein is an independent prognostic marker in hepatocellular carcinoma. *Cancer* 2009; **115**: 4576-4585.
16. Kim HM, Jung WH, Koo JS. Expression of Yes-associated protein (YAP) in metastatic breast cancer. *Int J Clin Exp Pathol* 2015; **8**: 11248-11257.
17. Zhang X, George J, Deb S, *et al.* The Hippo pathway transcriptional co-activator, YAP, is an ovarian cancer oncogene. *Oncogene* 2011; **30**: 2810-2822.
18. Coste B, Mathur J, Schmidt M, *et al.* Piezo1 and Piezo2 are essential components of distinct mechanically activated cation channels. *Science* 2010; **330**: 55-60.
19. Gudipaty SA, Lindblom J, Loftus PD, *et al.* Mechanical stretch triggers rapid epithelial cell division through Piezo1. *Nature* 2017; **543**: 118-121.
20. Pathak MM, Nourse JL, Tran T, *et al.* Stretch-activated ion channel Piezo1 directs lineage choice in human neural stem cells. *Proc Natl Acad Sci U S A* 2014; **111**: 16148-16153.
21. Li J, Hou B, Tumova S, *et al.* Piezo1 integration of vascular architecture with physiological force. *Nature* 2014; **515**: 279-282.
22. Yang XN, Lu YP, Liu JJ, *et al.* Piezo1 is as a novel trefoil factor family 1 binding protein that promotes gastric cancer cell mobility in vitro. *Dig Dis Sci* 2014; **59**: 1428-1435.
23. Han Y, Liu C, Zhang D, *et al.* Mechanosensitive ion channel Piezo1 promotes prostate cancer development through the activation of the Akt/mTOR pathway and acceleration of cell cycle. *Int J Oncol* 2019; **55**: 629-644.
24. McHugh BJ, Murdoch A, Haslett C, *et al.* Loss of the integrin-activating transmembrane protein Fam38A (Piezo1) promotes a switch to a reduced integrin-dependent mode of cell migration. *PLoS One* 2012; **7**: e40346.
25. Huang Z, Sun Z, Zhang X, *et al.* Loss of stretch-activated channels, PIEZOs, accelerates non-small cell lung cancer progression and cell migration. *Biosci Rep* 2019; **39**.
26. Duchemin AL, Vignes H, Vermot J. Mechanically activated piezo channels modulate outflow tract valve development through the Yap1 and Klf2-Notch signaling axis. *Elife* 2019; **8**: eLife.44706.

For Peer Review

27. Matsuo K, Ishibashi Y, Kobayashi I, *et al.* New human oral squamous carcinoma cell line and its tumorigenic subline producing granulocyte colony-stimulating factor. *Jpn J Cancer Res* 1994; **85**: 1257-1262.
28. Fujii S, Matsumoto S, Nojima S, *et al.* Arl4c expression in colorectal and lung cancers promotes tumorigenesis and may represent a novel therapeutic target. *Oncogene* 2015; **34**: 4834-4844.
29. Mikami Y, Fujii S, Nagata K, *et al.* GLI-mediated Keratin 17 expression promotes tumor cell growth through the anti-apoptotic function in oral squamous cell carcinomas. *J Cancer Res Clin Oncol* 2017; **143**: 1381-1393.
30. Miyoshi H, Blömer U, Takahashi M, *et al*. Development of a self-inactivating lentivirus vector. *J Virol* 1998; **72**: 8150-8157.
31. Fujii S, Shinjo K, Matsumoto S, *et al*. Epigenetic upregulation of ARL4C, due to DNA hypomethylation in the 3'-untranslated region, promotes tumorigenesis of lung squamous cell carcinoma. *Oncotarget* 2016; **7**: 81571-81587.
32. Matsumoto S, Kurimoto T, Taketo MM, *et al*. The WNT/MYB pathway suppresses KIT expression to control the timing of salivary proacinar differentiation and duct formation. *Development* 2016; **143**: 2311-2324.
33. Fujii S, Nagata K, Matsumoto S, *et al.* Wnt/β-catenin signaling, which is activated in odontomas, reduces Sema3A expression to regulate odontogenic epithelial cell proliferation and tooth germ development. *Sci Rep* 2019; **9**: 4257.
34. Takata T, Slootweg PJ. Tumours of the oral cavity and mobile tongue. Solan P, Gale N, Hunter K, *et al.* Malignant surface epithelial tumours. In WHO classification of head and neck tumours, (4th edn), El-Naggar AK,Chan JKC, Grandis JR, *et al.* (eds). IARC: Lyon, 2017; 108-111
35. O'Sullivan B. Head and Neck Tumours. In TNM Classification of Malignant Tumours, (8th edn), Brierley JD, Gospodarowicz MK, Wittekind C (eds). John Wiley & Sons, Ltd: Hoboken, 2017; 17-21.
36. Wang Z, Wu Y, Wang H, *et al*. Interplay of mevalonate and Hippo pathways regulates RHAMM transcription via YAP to modulate breast cancer cell motility. *Proc Natl Acad Sci U S A* 2014; **111**: E89-98.
37. Omori H, Nishio M, Masuda M, *et al*. YAP1 is a potent driver of the onset and progression of oral squamous cell carcinoma. *Sci Adv* 2020; **6**: eaay3324.
38. Yabuta N, Mukai S, Okada N, *et al.* The tumor suppressor Lats2 is pivotal in



For Peer Review

Aurora A and Aurora B signaling during mitosis. *Cell cycle* 2011; **10**: 2724-2736.

39. Oku Y, Nishiya N, Tazawa T*, et al.* Augmentation of the therapeutic efficacy of WEE1 kinase inhibitor AZD1775 by inhibiting the YAP-E2F1-DNA damage response pathway axis. *FEBS Open Bio* 2018; **8**: 1001-1012.
40. Fesquet D, De Bettignies G, Bellis M*, et al.* Binding of Kif23-iso1/CHO1 to 14-3-3 is regulated by sequential phosphorylations at two LATS kinase consensus sites. *PLos One* 2015; **10**: e0117857.
41. Zanconato F, Forcato M, Battilana G*, et al.* Genome-wide association between YAP/TAZ/TEAD and AP-1 at enhancers drives oncogenic growth. *Nat Cell Biol* 2015; **17**: 1218-1227.
42. Eisinger-Mathason TS, Mucaj V, Biju KM*, et al.* Deregulation of the Hippo pathway in soft-tissue sarcoma promotes FOXM1 expression and tumorigenesis. *Proc Natl Acad Sci U S A* 2015; **112**: E3402-3411.
43. Li Z, Razavi P, Li Q, *et al*. Loss of the FAT1 Tumor Suppressor Promotes Resistance to CDK4/6 Inhibitors via the Hippo Pathway. *Cancer cell* 2018; **34**: 893-905.
44. Zhang J, Ji JY, Yu M, *et al*. YAP-dependent induction of amphiregulin identifies a non-cell-autonomous component of the Hippo pathway. *Nat Cell Biol* 2009; **11**: 1444-1450.
45. Goto H, Nishio M, To Y, *et al*. Loss of Mob1a/b in mice results in chondrodysplasia due to YAP1/TAZ-TEAD-dependent repression of SOX9. *Development* 2018; **145**. dev159244.
46. Varelas X. The Hippo pathway effectors TAZ and YAP in development, homeostasis and disease. *Development* 2014; **141**: 1614-1626.
47. Stein C, Bardet AF, Roma G, *et al*. YAP1 Exerts Its Transcriptional Control via TEAD-Mediated Activation of Enhancers. *PLoS Genet* 2015; **11**: e1005465.
48. Syeda R, Xu J, Dubin AE*, et al.* Chemical activation of the mechanotransduction channel Piezo1. *Elife* 2015; **4**. eLife.07369.
49. Blythe NM, Muraki K, Ludlow MJ, *et al*. Mechanically activated Piezo1 channels of cardiac fibroblasts stimulate p38 mitogen-activated protein kinase activity and interleukin-6 secretion. *J Biol Chem* 2019; **294**: 17395-17408.
50. Sugimoto A, Miyazaki A, Kawarabayashi K*, et al.* Piezo type mechanosensitive ion channel component 1 functions as a regulator of the cell fate determination of

For Peer Review

mesenchymal stem cells. *Sci Rep* 2017; **7**: 17696.

51. Andolfo I, Rosato BE, Manna F, *et al*. Gain-of-function mutations in PIEZO1 directly impair hepatic iron metabolism via the inhibition of the BMP/SMADs pathway. *Am J Jematol* 2020; **95**: 188-197.
52. Zhang W, Liu HT. MAPK signal pathways in the regulation of cell proliferation in mammalian cells. *Cell Res* 2002; **12**: 9-18.
53. Cuadrado A, Nebreda AR. Mechanisms and functions of p38 MAPK signalling. *Biochem J* 2010; **429**: 403-417.
54. Lin YC, Guo YR, Miyagi A, *et al.* Force-induced conformational changes in PIEZO1. *Nature* 2019; **573**: 230-234.
55. Miyamoto T, Mochizuki T, Nakagomi H, *et al.* Functional role for Piezo1 in stretch-evoked $Ca^{2+}$ influx and ATP release in urothelial cell cultures. *J Biol Chem* 2014; **289**: 16565-16575.
56. Cancer Genome Atlas Network. Comprehensive genomic characterization of head and neck squamous cell carcinomas. *Nature* 2015; **517**: 576-582.
57. Elkabets M, Pazarentzos E, Juric D, *et al*. AXL mediates resistance to PI3Kα inhibition by activating the EGFR/PKC/mTOR axis in head and neck and esophageal squamous cell carcinomas. *Cancer cell* 2015; **27**: 533-546.

For Peer Review

**Table 1.** Relationship between the PIEZO1 intensity and clinicopathological characteristics of OSCC cases.

| | | PIEZO1 expression | | | *P* value |
|---|---|---|---|---|---|
| | | Negative | Weak | strong | |
| **Clinical T stage** | | | | | |
| T1 | 7 | 0 | 3 | 4 | |
| T2 | 20 | 0 | 13 | 7 | |
| T3 | 7 | 0 | 4 | 3 | |
| T4 | 11 | 0 | 2 | 9 | N.S.[a] |
| **Histologic grade** | | | | | |
| Well | 25 | 0 | 14 | 11 | |
| Moderately | 16 | 0 | 7 | 9 | |
| Poorly | 4 | 0 | 1 | 3 | N.S.[a] |
| **Lymph node metastasis** | | | | | |
| Positive | 11 | 0 | 4 | 7 | |
| Negative | 34 | 0 | 18 | 16 | N.S.[a] |

Abbreviations: Clinical T stage; *T1* tumor 2 cm or less in greatest dimension and 5 mm or less depth of invasion, *T2* tumor 2 cm or less in greatest dimension and more than 5 mm but no more than 10 mm depth of invasion or tumor more than 2 cm but not more than 4 cm in greatest dimension and depth of invasion no more than 10 mm, *T3* tumor more than 2 cm but not more than 4 cm in greatest dimension and depth of invasion more than 10 mm or tumor more than 4 cm in greatest dimension and not more than 10 mm depth of invasion, *T4* (*T4a and T4b*): *T4a* (*lip*) tumor invades through cortical bone, inferior alveolar nerve, floor of mouth, or skin (of the chin or nose), *T4a* (*oral cavity*) tumor more than 4 cm in greatest dimension and more than 10 mm depth of invasion or

For Peer Review

tumor invades through the cortical bone of the mandible or maxilla or involves the maxillary sinus, or invades the skin of the face, *T4b* (*lip and oral cavity*) tumor invades masticator space, pterygoid plates, or skull base, or encases internal carotid artery.

Histologic grade (WHO); *Grade 1* well differentiated, *Grade 2* moderately differentiated, *Grade 3* poorly differentiated.

[a] Statistical analyses were performed by Fisher's exact test. N.S.: not significant.

For Peer Review

**Table 2.** Relationship between the YAP expression and localization, and clinicopathological characteristics of OSCC cases.

| | | YAP expression and localization | | | *P* value |
|---|---|---|---|---|---|
| | | Negative | Nucleus/cytoplasm | Nucleus | |
| **Clinical T stage** | | | | | |
| T1 | 7 | 0 | 3 | 4 | |
| T2 | 20 | 1 | 5 | 14 | |
| T3 | 7 | 1 | 2 | 4 | |
| T4 | 11 | 0 | 3 | 8 | N.S.[a] |
| **Histologic grade** | | | | | |
| Well | 25 | 1 | 9 | 15 | |
| Moderately | 16 | 1 | 4 | 11 | |
| Poorly | 4 | 0 | 0 | 4 | N.S.[a] |
| **Lymph node metastasis** | | | | | |
| Positive | 11 | 2 | 4 | 5 | |
| Negative | 34 | 0 | 9 | 25 | N.S.[a] |

Abbreviations are same in the Table 1.

[a] Statistical analyses were performed by Fisher's exact test. N.S.: not significant.

For Peer Review

## Figure Legends

**Figure 1.** Proliferative capabilities of oral squamous cell carcinoma cells in the three-dimensional and suspension cultures.

(A) HSC-4 cells ($1 \times 10^5$ cells) and HSC-3 cells ($1 \times 10^5$ cells) were seeded in 2D, 3D (collagen or Matrigel) or suspension culture in the presence of 10% FBS for 48 h, and relative cell numbers were quantified using the CyQUANT cell proliferation assay. RFU: relative fluorescence units. (B) Gene enrichment analysis of down-regulated genes in suspension culture comparing with 2D culture for gene ontology biological processes was carried out. (C) HSC-4 cells were cultured in 2D or suspension culture for the indicated numbers of hours. Cell lysates were probed with anti-YAP/TAZ and anti-β-actin antibodies. Molecular weight size was noted referring to molecular weight marker. (D) *ANKRD1* and *CYR61* mRNA levels in HSC-4 cells cultured in 2D or suspension culture for 24 h were measured by quantitative RT-PCR. Relative levels of *ANKRD1* and *CYR61* mRNA expression were normalized to *GAPDH* and expressed as fold-changes compared with expression in 2D cells. (E) HSC-4 cells were transfected with control or LATS2 siRNA for 48 h, and then cells were cultured in 2D or suspension culture for 24 h. *ANKRD1* and *CYR61* mRNA levels were measured by quantitative RT-PCR. Relative levels of *ANKRD1* and *CYR61* mRNA expression were normalized to *GAPDH* and expressed as fold-changes compared with levels in 2D control cells. Results are shown as means ± s.d. of three independent experiments. **P*<0.05, ***P*<0.01. n.s.: not significant.

**Figure 2.** PIEZO1 is a transcriptional target of YAP signaling in oral squamous cell





For Peer Review

carcinoma cells.

(A) HSC-4 cells were cultured in 2D (UT), 2D (Coat) or 3D (collagen) culture for 24 h. *PIEZO1* mRNA levels were measured by quantitative RT-PCR. Relative levels of *PIEZO1* mRNA expression were normalized to *GAPDH* and expressed as fold-changes compared with expression in 2D (UT) cells. Cell lysates were probed with anti-PIEZO1 and anti-β-actin antibodies. Molecular weight size was noted referring to molecular weight marker. (B) HSC-4 cells were cultured in 2D or suspension culture for the indicated numbers of hours. *PIEZO1* mRNA levels were measured by quantitative RT-PCR. Relative levels of *PIEZO1* mRNA expression were normalized to *GAPDH* and expressed as fold-changes compared with expression in 2D cells. Cell lysates were probed with anti-PIEZO1 and anti-β-actin antibodies. Molecular weight size was noted referring to molecular weight marker. (C) HSC-4 cells were transfected with control or LATS2 siRNA for 48 h, and then cells were cultured in 2D or suspension culture for 24 h. *PIEZO1* mRNA levels were measured by quantitative RT-PCR. Relative levels of *PIEZO1* mRNA expression were normalized to *GAPDH* and expressed as fold-changes compared with expression in 2D control cells. (D) HSC-4 cells were transfected with control or two different YAP/TAZ siRNAs for 48 h, and then cells were cultured in 2D culture for 3 h. *PIEZO1* mRNA levels were measured by quantitative RT-PCR. Relative *PIEZO1* mRNA levels were normalized by *GAPDH* and expressed as fold-changes compared with levels in control siRNA transfected cells. (E) HSC-4 cells expressing mock or $YAP^{5SA}$ were cultured in 2D or suspension culture for 24 h and *PIEZO1* mRNA levels were measured by quantitative RT-PCR (left panel). Relative levels of *PIEZO1* mRNA expression were

For Peer Review

normalized to *GAPDH* and expressed as fold-changes compared with expression in 2D control cells. Cell lysates were probed with anti-PIEZO1, anti-YAP/TAZ and anti-β-actin antibodies (right panel). Molecular weight size was noted referring to molecular weight marker. Arrowhead indicates non-specific bands. (F) Chromatin from HSC-4 cells expressing mock or $YAP^{5SA}$ was immunoprecipitated with anti-control IgG or anti-TEAD4 and anti-FLAG antibodies, and the precipitates were analyzed by PCR for TEAD4 binding site 1, site 2 or site 3 of the *PIEZO1* gene. White box indicates TEAD4 binding motif and site 3 has two TEAD4 binding motifs. Results are shown as means ± s.d. of three independent experiments. **P*<0.05, ***P*<0.01. n.s.: not significant.

**Figure 3.** PIEZO1 expression is involved in agonist-induced ERK1/2 and p38 MAPK activation.

(A) *PIEZO1* mRNA levels were measured in OSCC cell lines (HSC-4, HSC-3, HSC-2, SAS, MISK81-5 and sMISK cells) by quantitative RT-PCR. Relative levels of *PIEZO1* mRNA expression were normalized to *GAPDH* and expressed as fold-changes compared with expression in control MKN-45 cells. (B) HSC-4 cells were pre-loaded with Fluo-4-AM and were exposed without or with 1 and 10 μM Yoda1. Then, intracellular $Ca^{2+}$ influx at 160 sec was measured. RFU: relative fluorescence units. (C) HSC-4 cells were transfected with control or two different PIEZO1 siRNAs for 48 h, and *PIEZO1* mRNA levels were measured by quantitative RT-PCR. Relative *PIEZO1* mRNA levels were normalized by *GAPDH* and expressed as fold-changes compared with levels in control siRNA transfected cells. Cell lysates were probed with anti-PIEZO1 and anti-β-actin

For Peer Review

antibodies. Molecular weight size was noted referring to molecular weight marker. (D) HSC-4 cells transfected with control or two different PIEZO1 siRNAs were pre-loaded with Fluo-4-AM and were exposed without or with 10 μM Yoda1. Then, intracellular $Ca^{2+}$ influx at 160 sec was measured. RFU: relative fluorescence units. (E) HSC-4 cells were transfected with control or two different PIEZO1 siRNAs, and treated without or with 10 μM Yoda1 for 5 min. Cell lysates were probed with anti-phospho-ERK1/2, anti-ERK1/2, anti-phospho-p38, anti-p38, anti-phospho-AKT and anti-pan-AKT antibodies. Molecular weight size was noted referring to molecular weight marker. Results are shown as means ± s.d. of three independent experiments. **P*<0.05, ***P*<0.01. n.s.: not significant.

**Figure 4.** PIEZO1 expression is required for cell proliferation in oral squamous cell carcinoma cells.

(A) HSC-4 cells were transfected with control or PIEZO1 #1 siRNA for 48 h. The cells were stained with anti-Ki-67 antibody and Hoechst 33342, and then Ki-67-positive cells and Hoechst 33342-stained cells were counted, respectively. Results are expressed as the percentage of Ki-67-positive cells compared with total Hoechst 33342-stained cells. (B) HSC-4 cells were transfected with control or two different PIEZO1 siRNAs. The cells were cultured in the presence of 5% FBS for the indicated numbers of days, and cell numbers were counted. (C) HSC-4 cells were cultured without or with 100 μM GsMTx-4 in the absence of FBS for 48 h, and relative cell numbers were quantified using the CyQUANT cell proliferation assay. RFU: relative fluorescence units. (D) *PIEZO1*



For Peer Review

mRNA levels in HSC-4 cells expressing control or PIEZO1 #1 and #2 shRNAs were measured by quantitative RT-PCR. Relative levels of *PIEZO1* mRNA expression were normalized to *GAPDH* and expressed as fold-changes compared with expression in control cells. Lysates of HSC-4 cells expressing control or PIEZO1 #1 and #2 shRNAs were probed with anti-PIEZO1 and anti-β-actin antibodies. Molecular weight size was noted referring to molecular weight marker. (E) HSC-4 cells expressing control or PIEZO1 #1 and #2 shRNAs were pre-loaded with Fluo-4-AM and were exposed without or with 10 μM Yoda1. Then, intracellular $Ca^{2+}$ influx at 160 sec was measured. RFU: relative fluorescence units. (F) HSC-4 cells expressing control or PIEZO1 #1 and #2 shRNAs were transfected with control or LATS2 siRNA for 48 h, and then cells were cultured for 4 days in the 3D Matrigel. The cells were stained with anti-Ki-67 antibody and Hoechst 33342, and then Ki-67-positive cells and Hoechst 33342-stained cells were counted, respectively. Results are expressed as the percentage of Ki-67-positively stained cells compared with total Hoechst 33342-stained cells ($n$ = 13,469). (G) HSC-4 cells expressing control or PIEZO1 #1 and #2 shRNAs were transfected with mock or $YAP^{5SA}$, and then cells were cultured for 4 days in the 3D Matrigel. The cells were stained with anti-Ki-67 antibody and Hoechst 33342, and then Ki-67-positive cells and Hoechst 33342-stained cells were counted, respectively. Results are expressed as the percentage of Ki-67-positively stained cells compared with total Hoechst 33342-stained cells ($n$ = 5,603). Results are shown as means ± s.d. of three independent experiments. *$P$<0.05, **$P$<0.01. Scale bars, 100 μm.

For Peer Review

**Figure 5.** PIEZO1 and YAP are expressed in human oral squamous cell carcinoma tissues. (A) Oral squamous cell carcinoma tissues (*n* = 45) were stained with anti-PIEZO1 antibody and hematoxylin. PIEZO1-positive signal intensity was classified as follows: negative; weak; strong. Percentages of three groups based on PIEZO1-positive signal intensity in the non-tumor regions and the tumor lesions are shown in the panel. Boxes show enlarged images. (B) Oral squamous cell carcinoma tissues (*n* = 45) were stained with anti-PIEZO1, anti-YAP and anti-Ki-67 antibodies, and hematoxylin. Solid boxes show enlarged images. Numbers of cases with YAP-positive in non-tumor region or tumor lesion, and PIEZO1 intensity strong or negative/weak was shown. Scale bars, 500 μm (A), 100 μm (B).

For Peer Review

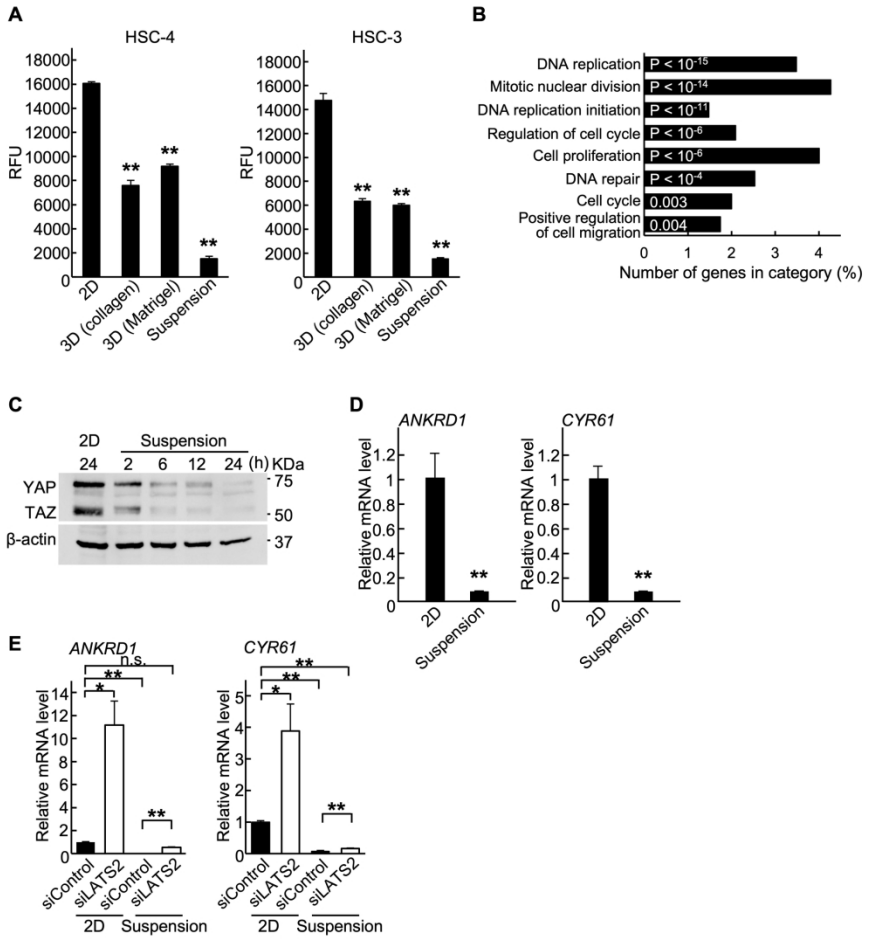


Figure 1. Proliferative capabilities of oral squamous cell carcinoma cells in the three-dimensional and suspension cultures.

190x254mm (300 x 300 DPI)

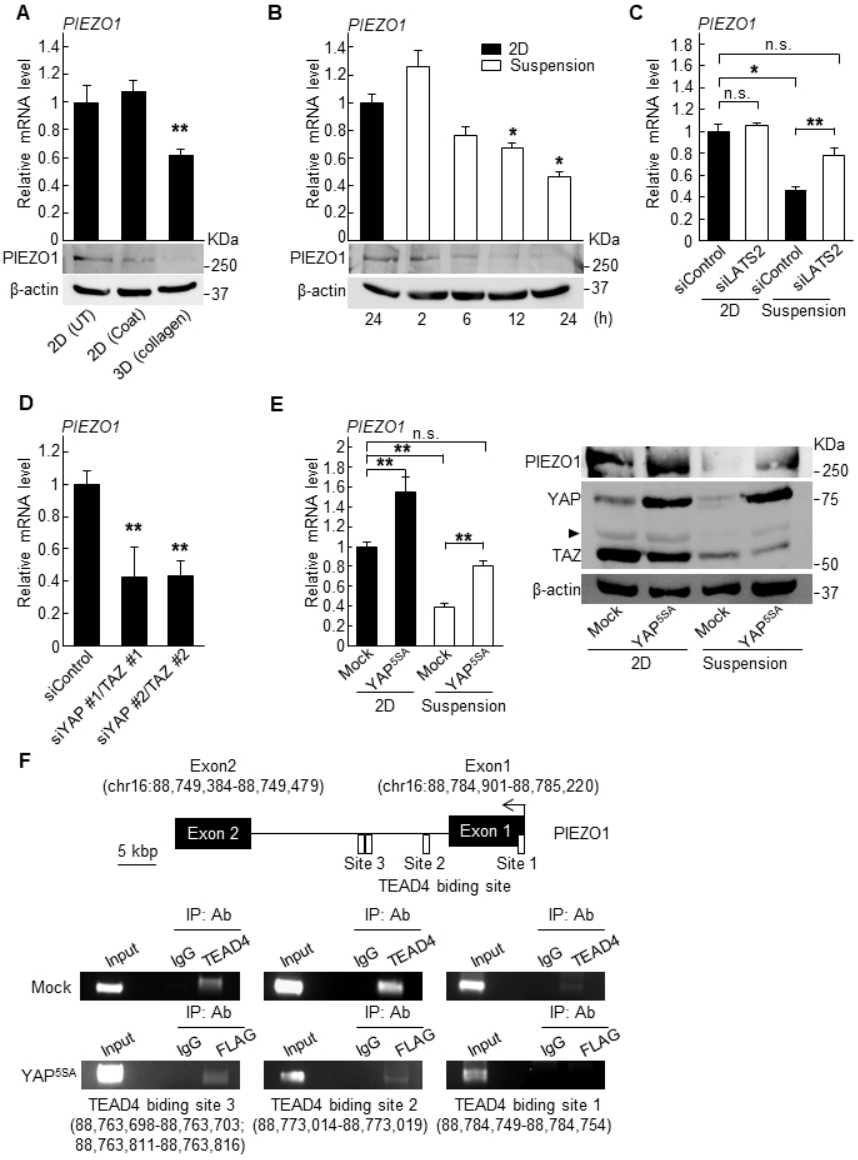


Figure 2. PIEZO1 is a transcriptional target of YAP signaling in oral squamous cell carcinoma cells.

190x254mm (96 x 96 DPI)

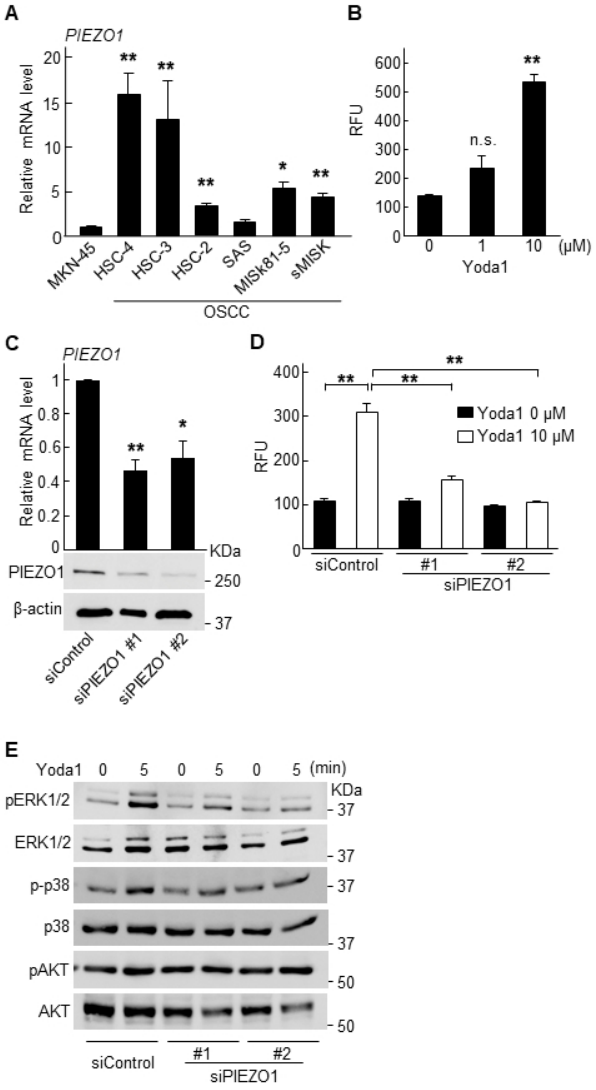


Figure 3. PIEZO1 expression is involved in agonist-induced ERK1/2 and p38 MAPK activation.

190x254mm (96 x 96 DPI)

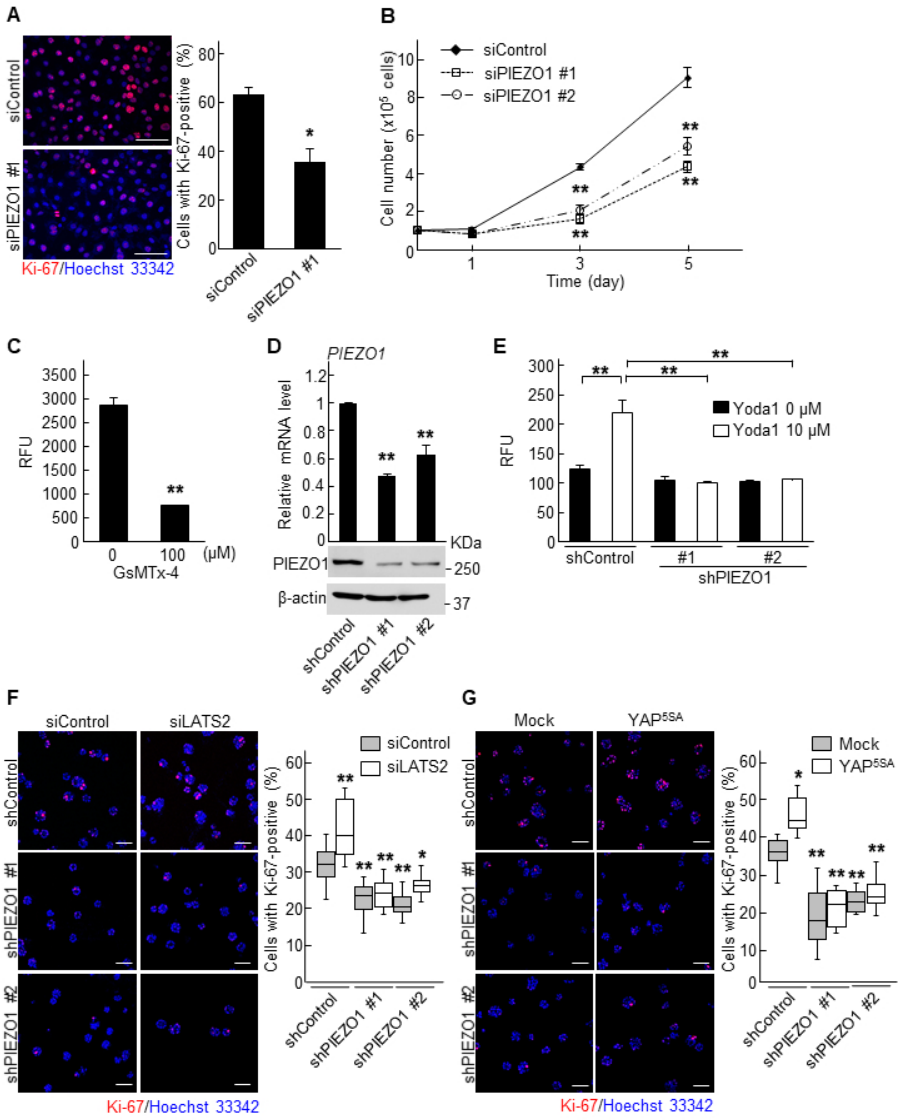


Figure 4. PIEZO1 expression is required for cell proliferation in oral squamous cell carcinoma cells.

190x254mm (96 x 96 DPI)

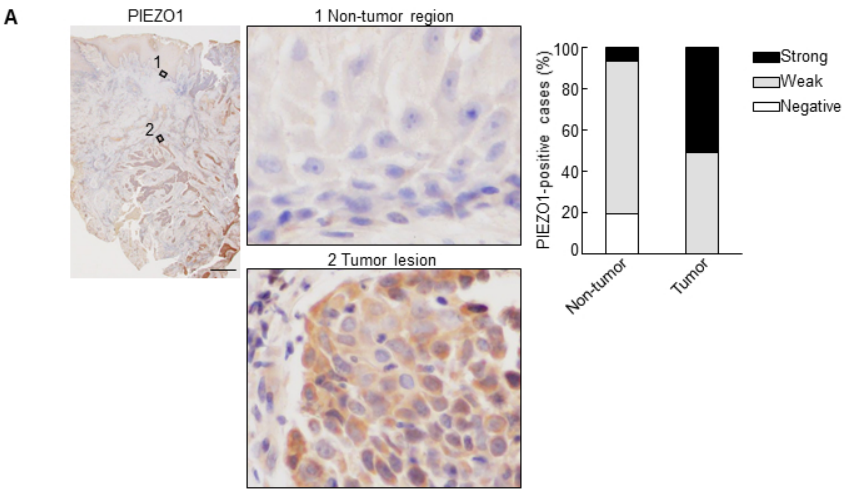


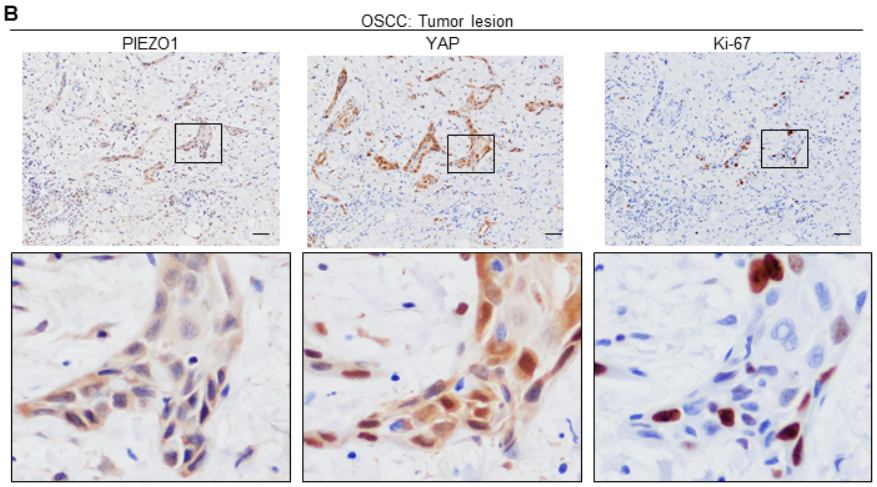


| | | YAP-positive cases | |
|---|---|---|---|
| | | Non-tumor region | Tumor lesion |
| PIEZO1 intensity | Strong | 1/10 (10 %) | 22/43 (51.2 %) |
| | Negative/Weak | 9/10 (90 %) | 21/43 (48.8 %) |
| | Total | 10 | 43 |

Figure 5. PIEZO1 and YAP are expressed in human oral squamous cell carcinoma tissues.

190x254mm (96 x 96 DPI)

# Supporting Information

## YAP signaling induces PIEZO1 expression to promote oral squamous cell carcinoma cell proliferation

Kana Hasegawa[1], Shinsuke Fujii[1*], Shinji Matsumoto[2], Yudai Tajiri[1,3], Akira Kikuchi[2] and Tamotsu Kiyoshima[1]

[1]Laboratory of Oral Pathology, Division of Maxillofacial Diagnostic and Surgical Sciences, Faculty of Dental Science, Kyushu University, 3-1-1 Maidashi, Higashi-ku, Fukuoka 812-8582, Japan

[2]Department of Molecular Biology and Biochemistry, Graduate School of Medicine, Osaka University, 2-2 Yamadaoka, Suita 565-0871, Japan

[3]Department of Dentistry and Oral Surgery, Clinical Research Institute, National Hospital Organization Kyushu Medical Center, 1-8-1 Jigyohama, Chuo-ku, Fukuoka 810-8563, Japan

[*]Corresponding author. Laboratory of Oral Pathology, Division of Maxillofacial Diagnostic and Surgical Sciences, Faculty of Dental Science, Kyushu University

3-1-1 Maidashi, Higashi-ku, Fukuoka 812-8582, Japan

Phone: +81-92-642-6328; Fax: +81-92-642-6329

E-mail: sfujii@dent.kyushu-u.ac.jp

For Peer Review

## Supplementary Materials and methods

### Cell lines and reagents

Anti-PIEZO1 polyclonal antibody (15939-1-AP) (for western blotting and immunohistochemistry) was obtained from Proteintech (Rosemont, IL, USA). Anti-YAP/TAZ (8418S) (for western blotting and immunocytochemistry), anti-phospho-ERK1/2 (4370S), anti-ERK1/2 (4695S), anti-phospho-AKT (4060S), anti-pan-AKT (4691S) (for western blotting) and anti-cleaved caspase-3 (9664S) (for immunocytochemistry) antibodies were obtained from Cell Signaling Technology (Beverly, MA, USA). Anti-Ki-67 (ab15580) and anti-PCNA (ab92552) (for immunocytochemistry and immunohistochemistry) antibodies were from Abcam (Cambridge, UK). Anti-YAP (sc-101199) (for immunohistochemistry) antibody was from Santa Cruz Biotechnology (Dallas, TX, USA). Anti-phospho-p38 (612280) and anti-p38 (612168) (for western blotting) antibodies were from BD Biosciences (San Jose, CA, USA). Anti-β-actin (A5441) (for western blotting) antibody was from Sigma-Aldrich (Steinheim, Germany). Type I collagen solution was purchased from Nippi, Inc. (Tokyo, Japan). Phalloidin, and Simvastatin and Yoda1 were from Invitrogen and Sigma-Aldrich, respectively. GsMTx-4 was from Abcam.

### Plasmid construction and infection using lentivirus harboring a cDNA or shRNA

To generate OSCC cells that stably express $YAP^{5SA}$ or PIEZO1 shRNA, parental cells (5 × $10^4$ cells/well in a 12-well plate) were treated with lentivirus and 10 μg/ml polybrene.





For Peer Review

The cells were then centrifuged at 1080 × g for 1 h, and incubated for another 24 h. The cells that demonstrated stable expression of $YAP^{5SA}$, PIEZO1 #1 or #2 shRNA, were selected and maintained in culture medium containing 5 μg/ml Blasticidin S (FUJIFILM Wako Pure Chemical Corporation, Osaka, Japan) [1].

**Chromatin immunoprecipitation (ChIP) assay**

ChIP assay was performed as described previously [2]. HSC-4 cells expressing Mock or $YAP^{5SA}$ were cross-linked with 1% (v/v) formaldehyde for 20 min at room temperature. The cells were lysed with sodium dodecyl sulfate (SDS) lysis buffer (50 mM Tris-HCl (pH 8.0), 10 mM EDTA, and 0.5% (w/v) SDS) and sonicated to shear DNA to a size range between 200 and 1000 bp. Sheared chromatin samples were diluted in ChIP dilution buffer (16.7 mM Tris-HCl (pH 8.0), 167 mM NaCl, 1.2 mM EDTA, and 1.1% (w/v) Triton X-100) supplemented with protease inhibitors, and precleared with salmon sperm DNA/protein A-agarose (Millipore) and incubated for 4 h at 4˚C with 10 μg of anti-TEAD4 (ab58310, Abcam), anti-FLAG (F1804, Sigma) or negative control IgG (5415S, Cell Signaling Technology). Immunocomplexes were absorbed with salmon sperm DNA/protein A-agarose beads, and washed once with high salt buffer (20 mM Tris-HCl (pH 8.1), 500 mM NaCl, 0.1% (w/v) SDS, 1% (w/v) TritonX-100, and 2 mM EDTA), once with LiCl buffer (10 mM Tris-HCl (pH 8.1), 0.25 M LiCl, 1 mM EDTA, 1% (w/v) deoxycholic acid, and 1% (w/v) Nonidet P-40), and three times with TE buffer (10 mM Tris-HCl (pH 8.1), and 1 mM EDTA). Immune complexes extracted in elution buffer (1% (w/v) SDS and 100 mM $NaHCO_3$) were incubated for 4 h at 65°C to revert DNA-protein





For Peer Review

cross-links. Then the DNA was extracted by incubation in proteinase K (final concentration of 50 mg/ml) buffer for 1 h at 45°C. The purified DNA was used in PCR to assess the presence of target sequences. Forward and reverse primers were as follows: fragment containing TEAD4-binding site 1, 5'-GCGCTCATGCTTCAGGAATGC-3' and 5'-CTGCTGGCTGGTGAGTGG-3; TEAD4-binding site 2, 5'-TGCCTGGAAGACTGTGTCAG-3' and 5'-AATGAGACCCAGGAGGAAGGAG-3; TEAD4-binding site 3, 5'-TAGGTGCTCCCTGACACTCTCTG-3' and 5'-CCAAAGCCTTCATTTCAGGA-3; ANKRD1-binding site, 5'-GAGGGGAGGACAAGCTAACC-3' and 5'-CGATGTGATCACCACCAAAG-3 [3].

**Intracellular calcium measurement**

To examine agonist-dependent $Ca^{2+}$ influx, cells were loaded with Calcium Kit-Fluo-4 AM (FUJIFILM Wako) for 1 h at 37°C according to the manufacturer's instructions [4]. The measurements were performed with FlexStation 3 microplate reader using the 'Flex' read mode, and images at 485 nm excitation/525 nm emission were collected every 2 sec. After the cells were stimulated by compound, fluorescence measurements were carried out for 5 min. And then, we confirmed the vitality of the cells, in which propidium iodide (PI) (Wako) was not stained (data not shown).

**Immunocytochemistry**

For Peer Review

HSC-4 cells were fixed in 4% paraformaldehyde (PFA) in PBS for 30 min at room temperature. After cells were permeabilized in PBS containing 0.5% (w/v) Triton X-100 and 40 mg/ml BSA (Wako) for 30 min at room temperature, and then blocked with 0.2% BSA to prevent non-specific binding for 30 min at room temperature. The cells were incubated with primary antibodies (used at 1:100 for Ki-67, used at 1:300 for PCNA, used at 1:400 for cleaved caspase-3) at 4°C overnight, and then incubated with secondary antibodies for 3 h at room temperature. Cell nuclei were counterstained with 4', 6-diamidino-2-phenylindole dihydrochloride (DAPI) (Dojindo, Kumamoto, Japan) or Hoechst 33342 (Dojindo) for 15 min at room temperature [5]. The samples were viewed with Z-X800 fluorescence microscope (Keyence, Osaka, Japan).

**Immunohistochemistry**

Immunohistochemical staining was performed on 5-μm-thick paraffin sections. Antigen retrieval, elimination of the endogenous peroxide activity, and blocking were carried out as previously described [4]. Then the sections were reacted with each primary antibody (used at 1:250 for PIEZO1, used at 1:100 for YAP, used at 1:300 for Ki-67, used at 1:500 for PCNA) at 4°C overnight. The sections were incubated with secondary antibody (Histofine Simple Stain MAX PO, Nichirei, Tokyo, Japan) for 1 h at RT. The immunoreactivity was visualized with a solution of DAB substrate solution. Subsequently, the sections were counterstained with hematoxylin.

**Microarray analysis**

For Peer Review

Microarray analyses were performed using HSC-4 cells cultured in 2D culture or suspension culture as previously described [5]. 1 μg of total RNA was used for microarray analysis. The mRNA expression profile was produced by Cell Innovator Inc. (Fukuoka, Japan) using gene microarray technology (SurePrint G3 Human Gene Expression Microarray 8 × 60 K v3, Agilent Technologies, Santa Clara, CA, USA). The raw data reported in this study was deposited in NCBI GEO under accession number (GSE150044). Gene Ontology (GO) analysis was performed using DAVID database (http://david.abcc.ncifcrf.gov/).

For Peer Review

## SUPPLEMENTAL REFERENCES


1. Matsumoto S, Fujii S, Sato A*, et al.* A combination of Wnt and growth factor signaling induces Arl4c expression to form epithelial tubular structures. *EMBO J* 2014; **33**: 702-718.
2. Matsumoto S, Kurimoto T, Taketo MM, *et al*. The WNT/MYB pathway suppresses KIT expression to control the timing of salivary proacinar differentiation and duct formation. *Development* 2016; **143**: 2311-2324.
3. Stein C, Bardet AF, Roma G, *et al*. YAP1 Exerts Its Transcriptional Control via TEAD-Mediated Activation of Enhancers. *PLoS Genet* 2015; **11**: e1005465.
4. Fujii S, Tajiri Y, Hasegawa K*, et al.* The TRPV4-AKT axis promotes oral squamous cell carcinoma cell proliferation via CaMKII activation. *Lab Invest* 2020; **100**: 311-323.
5. Fujii S, Nagata K, Matsumoto S*, et al.* Wnt/β-catenin signaling, which is activated in odontomas, reduces Sema3A expression to regulate odontogenic epithelial cell proliferation and tooth germ development. *Sci Rep* 2019; **9**: 4257.


For Peer Review

**Supplementary Figure Legends**

**Supplementary Figure 1.** The effect of YAP/TAZ signaling on OSCC cells.

(A) HSC-4 cells were transfected with control or two different YAP/TAZ siRNAs for 48 h. Cell lysates were probed with anti-YAP/TAZ and anti-β-actin antibodies (upper left panel). Molecular weight size was noted referring to molecular weight marker. *ANKRD1* and *CYR61* mRNA levels in the cells were also measured by quantitative RT-PCR. Relative levels of *ANKRD1* and *CYR61* mRNA expression were normalized to *GAPDH* and expressed as fold-changes compared with levels in control siRNA transfected cells (upper middle panels). The cells were cultured in the presence of 5% FBS for 48 h, and relative cell numbers were quantified using the CyQUANT cell proliferation assay (upper right panel). RFU: relative fluorescence units. HSC-4 cells were cultured without or with 1 and 2 μM Simvastatin. The cells were cultured in the presence of 5% FBS for the indicated numbers of days, and cell numbers were counted (lower left panel). *ANKRD1* and *CYR61* mRNA levels in the cells were also measured by quantitative RT-PCR. Relative levels of *ANKRD1* and *CYR61* mRNA expression were normalized to *GAPDH* and expressed as fold-changes compared with levels in control siRNA transfected cells (lower right panel). (B) *ANKRD1* and *CYR61* mRNA levels in HSC-3 and MISK81-5 cells cultured in 2D or suspension culture for 24 h were measured by quantitative RT-PCR. Relative levels of *ANKRD1* and *CYR61* mRNA expression were normalized to *GAPDH* and expressed as fold-changes compared with expression in 2D cells. (C) HSC-4 cells were transfected with control or LATS2 siRNA for 48 h, and *LATS2* mRNA levels were measured by quantitative RT-PCR. Relative *LATS2* mRNA levels were normalized

For Peer Review

by *GAPDH* and expressed as fold-changes compared with levels in control siRNA transfected cells. (D) HSC-4 cells were transfected with control or LATS2 siRNA for 48 h, and then cells were cultured in 2D or suspension culture for 24 h. *AURKB* and *FOXM1* mRNA levels were measured by quantitative RT-PCR. Relative levels of *AURKB* and *FOXM1* mRNA expression were normalized to *GAPDH* and expressed as fold-changes compared with levels in 2D control cells. Results are shown as means ± s.d. of three independent experiments. **P*<0.05, ***P*<0.01. n.s.: not significant.

**Supplementary Figure 2.** YAP signaling regulates PIEZO1 expression in OSCC cells. (A) The expression of *PIEZO1, PIEZO2, AREG* or *CDK6* in 518 tumor lesions and 44 non-tumor regions in head and neck region was evaluated using TCGA dataset. Correlation between *PIEZO1* and *AREG* or *CDK6* mRNA was examined in the tumor lesion. RPKM, reads per kilobase per million reads. Spearman's rank rho was used to calculate the "r" correlation coefficient. (B) *PIEZO1* mRNA levels in HSC-3 and MISK81-5 cells cultured in 2D or suspension culture for 24 h were measured by quantitative RT-PCR. Relative levels of *PIEZO1* mRNA expression were normalized to *GAPDH* and expressed as fold-changes compared with expression in 2D cells. (C) HSC-3 cells were transfected with control or two different YAP/TAZ siRNAs for 48 h, and then cells were cultured in 2D culture for 3 h. *PIEZO1* mRNA levels were measured by quantitative RT-PCR. Relative *PIEZO1* mRNA levels were normalized by *GAPDH* and expressed as fold-changes compared with levels in control siRNA transfected cells (left panel). HSC-3 cells expressing mock or $YAP^{5SA}$ were cultured in 2D or suspension culture





For Peer Review

for 24 h and *PIEZO1* mRNA levels were measured by quantitative RT-PCR. Relative levels of *PIEZO1* mRNA expression were normalized to *GAPDH* and expressed as fold-changes compared with expression in 2D control cells (right panel). (D) HSC-4 cells expressing mock or $YAP^{5SA}$ were cultured in 2D or suspension culture for 24 h, and *ANKRD1* and *CYR61* mRNA levels were measured by quantitative RT-PCR. Relative levels of *ANKRD1* and *CYR61* mRNA expression were normalized to *GAPDH* and expressed as fold-changes compared with expression in 2D control cells. (E) Genomic views of TEAD1, TEAD4, H3K27ac and H3K9ac ChIP enrichment at human *PIEZO1* gene obtained from Cistrome Data Browser database. The *PIEZO1* gene enhancer region contains three predicted TEAD4-binding sites. Chromatin from HSC-4 cells expressing mock was immunoprecipitated with anti-control IgG or anti-TEAD4 antibody, and the precipitates were analyzed by PCR for TEAD4 binding site of the *ANKRD1* gene promoter. Results are shown as means ± s.d. of three independent experiments. **P*<0.05, ***P*<0.01. n.s.: not significant.

**Supplementary Figure 3.** The effect of PIEZO1 on YAP/TAZ signaling.

(A) The expression of *PIEZO1* and *PIEZO2* in cell lines was evaluated using Cancer Cell Line Encyclopedia dataset. (B) *PIEZO2* mRNA levels were measured in OSCC cell lines (HSC-4, HSC-3, HSC-2, SAS, MISK81-5 and sMISK cells), A549 and MKN-45 cells by quantitative RT-PCR. Relative levels of *PIEZO2* mRNA expression were normalized to *GAPDH* and expressed as fold-changes compared with expression in control A549 cells. (C) HSC-4 cells were pre-loaded with Fluo-4-AM and were exposed without or with 1





For Peer Review

and 10 μM Yoda1. Then, intracellular $Ca^{2+}$ influx was measured. RFU: relative fluorescence units. (D) HSC-4 cells were transfected with control or two different PIEZO1 siRNAs for 48 h, and *PIEZO2*, *ANKRD1* and *CYR61* mRNA levels were measured by quantitative RT-PCR. Relative *PIEZO2*, *ANKRD1* and *CYR61* mRNA levels were normalized by *GAPDH* and expressed as fold-changes compared with levels in control siRNA transfected cells (upper panels). HSC-4 cells were transfected with control or two different PIEZO1 siRNAs for 48 h, and the cells were stained with anti-YAP/TAZ antibody, phalloidin and Hoechst 33342. Cells with nuclear YAP/TAZ are expressed as the percentage of YAP/TAZ-positively stained cells compared with total Hoechst 33342-stained cells ($n$ = 1,516) (lower panels). (E) HSC-4 cells transfected with control or two different PIEZO1 siRNAs were pre-loaded with Fluo-4-AM and were exposed without or with 10 μM Yoda1. Then, intracellular $Ca^{2+}$ influx was measured. RFU: relative fluorescence units. Results are shown as means ± s.d. of three independent experiments. Scale bars, 100 μm. n.s.: not significant.

**Supplementary Figure 4.** PIEZO1 regulates cell proliferation of OSCC cells.

(A) HSC-4 cells were transfected with control or PIEZO1 #1 siRNA for 48 h. The cells were stained with anti-PCNA antibody and Hoechst 33342, and then PCNA-positive cells and Hoechst 33342-stained cells were counted, respectively. Results are expressed as the percentage of PCNA-positive cells compared with total Hoechst 33342-stained cells. (B) HSC-4 cells were transfected with control or PIEZO1 #1 siRNA for 48 h. The cells were stained with anti-cleaved caspase-3 antibody and DAPI. (C) HSC-4 cells expressing





For Peer Review

control or PIEZO1 #1 and #2 shRNAs were pre-loaded with Fluo-4-AM and were exposed without or with 10 μM Yoda1. Then, intracellular $Ca^{2+}$ influx was measured. RFU: relative fluorescence units. (D) HSC-4 cells expressing control or PIEZO1 #1 and #2 shRNAs were transfected with control or LATS2 siRNA for 48 h (left panels) or with mock or $YAP^{5SA}$ expression (right panels), and then cells were cultured for 4 days in the 3D Matrigel. The cells were stained with anti-PCNA antibody and Hoechst 33342, and then PCNA-positive cells and Hoechst 33342-stained cells were counted, respectively. Results are expressed as the percentage of PCNA-positively stained cells compared with total Hoechst 33342-stained cells ($n$ = 14,242). (E) HSC-4 cells expressing PIEZO1 #1 and #2 shRNAs were transfected with control or LATS2 siRNA for 48 h (left panels) or with mock or $YAP^{5SA}$ expression (right panels), and then cells were cultured in 2D or suspension culture for 24 h. *PIEZO1* or *ANKRD1* mRNA levels were measured by quantitative RT-PCR. Relative *PIEZO1* or *ANKRD1* mRNA levels were normalized by *GAPDH* and expressed as fold-changes compared with levels in 2D control cells. Results are shown as means ± s.d. of three independent experiments. *$P$<0.05, **$P$<0.01. Scale bars, 100 μm. n.s.: not significant.

**Supplementary Figure 5.** PIEZO1 is expressed in human oral squamous cell carcinoma tissues.

Oral squamous cell carcinoma tissues ($n$ = 45) were stained with anti-PIEZO1 antibody and hematoxylin. PIEZO1-positive signal intensity was classified as follows: negative; weak; strong. Boxes show enlarged images. Scale bars, 100 μm.

For Peer Review

**Supplementary Figure 6.** YAP is expressed in human oral squamous cell carcinoma tissues.

(A) Oral squamous cell carcinoma tissues ($n$ = 45) were stained with anti-YAP antibody and hematoxylin. YAP expression and localization were classified as follows: negative; nucleus/cytoplasm; nucleus. Boxes show enlarged images. (B) Percentages of three groups based on the YAP expression and localization in the tumor lesions and the non-tumor regions are shown in the panel. (C) Oral squamous cell carcinoma tissues ($n$ = 45) were stained with anti-YAP, anti-PIEZO1 and anti-Ki-67 antibodies, and hematoxylin. Box shows enlarged images. Scale bars, 50 μm.

**Supplementary Figure 7.** Co-expression of PIEZO1, YAP, Ki-67 and PCNA in human oral squamous cell carcinoma tissues.

Oral squamous cell carcinoma tissues ($n$ = 45) were stained with anti-PIEZO1, anti- YAP, anti-Ki-67 and anti-PCNA antibodies, and hematoxylin. Representative data (n = 5) are shown. Scale bars, 20 μm.

For Peer Review

**Table S1.** Designs for siRNAs used in this study.

| siRNA | Sequence |
|---|---|
| human YAP #1 | Sense: GACAUCUUCUGGUCAGAGATT<br>Antisense: UCUCUGACCAGAAGAUGUCTT |
| human YAP #2 | Sense: GCUCAUUCCUCUCCAGCUUTT<br>Antisense: AAGCUGGAGAGGAAUGAGCTT |
| human TAZ #1 | Sense: AGGUACUUCCUCAAUCACATT<br>Antisense: UGUGAUUGAGGAAGUACCUTT |
| human TAZ #2 | Sense: CCCAACAGACCCGUUUCCCUGAUUUTT<br>Antisense: AAAUCAGGGAAACGGGUCUGUUGGGTT |
| human LATS2 | Sense: GCCACGACUUAUUCUGGAATT<br>Antisense: UUCCAGAAUAAGUCGUGGCTT |
| human PIEZO1 #1 | Sense: AGAAGAAGAUCGUCAAGUATT<br>Antisense: UACUUGACGAUCUUCUUCUTT |
| human PIEZO1 #2 | Sense: CCAACCUCAUCAGCGACUUTT<br>Antisense: AAGUCGCUGAUGAGGUUGGTT |
| Randomized control | Sense: CAGUCGCGUUUGCGACUGGTT<br>Antisense: CCAGUCGCAAACGCGACUGTT |

For Peer Review

**Table S2.** Quantitative RT-PCR primers used in this study.

| Gene | Primers |
|---|---|
| human LATS2 | Forward 5′-GCGATTCGTTTGCGTCCTAC-3′<br>Reverse 5′-CCGGGGAAAAGGTAGTCCAC-3′ |
| human PIEZO1 | Forward 5′-AGGAACAGGCAGGACAGCTA-3′<br>Reverse 5′-GCGTGTCAGCTCATCCACTA-3′ |
| human PIEZO2 | Forward 5′-GACGACTCTGCAGGCAAGAA-3′<br>Reverse 5′-AGAAGAGCAGCAGAAATCGGG-3′ |
| human ANKRD1 | Forward 5′-ACGCCAAAGACAGAGAAGGA-3′<br>Reverse 5′-TTCTGCCAGTGTAGCACCAG-3′ |
| human CYR61 | Forward 5′-TCCGAGGTGGAGTTGACGAG-3′<br>Reverse 5′-AGCACTGGGACCATGAAGTTG-3′ |
| human AURKB | Forward 5′-CCTCCCTGAGGAGGAAGACA-3′<br>Reverse 5′-TGCACCACAGATCCACCT TC-3′ |
| human FOXM1 | Forward 5′-GTTTATCAGTGCTGCTAGCTGAGG-3′<br>Reverse 5′-CAGGCTGGATTTCTTCCTCCTTG-3′ |
| human GAPDH | Forward 5′-GCACCGTCAAGGCTGAGAAC-3′<br>Reverse 5′-TGGTGAAGACGCCAGTGGA-3′ |

For Peer Review

Table S3. Gene enrichment analysis in HSC-4 cells.

| Term | Count | % | *p*-Value |
|---|---|---|---|
| DNA replication | 40 | 3.487358 | 1.53E-16 |
| G1/S transition of mitotic cell cycle | 32 | 2.789887 | 7.64E-16 |
| rRNA processing | 46 | 4.010462 | 1.28E-15 |
| Mitotic nuclear division | 49 | 4.272014 | 4.49E-15 |
| Cell division | 59 | 5.143854 | 8.91E-15 |
| Sister chromatid cohesion | 30 | 2.615519 | 5.89E-14 |
| DNA replication initiation | 17 | 1.482127 | 1.00E-12 |
| Regulation of transcription involved in G1/S transition of mitotic cell cycle | 11 | 0.959024 | 1.07E-07 |
| Regulation of cell cycle | 24 | 2.092415 | 1.42E-07 |
| Cell proliferation | 46 | 4.010462 | 1.46E-07 |
| Chromosome segregation | 17 | 1.482127 | 3.99E-07 |
| De novo' IMP biosynthetic process | 6 | 0.523104 | 2.44E-06 |
| DNA unwinding involved in DNA replication | 7 | 0.610288 | 3.94E-06 |
| Purine nucleotide biosynthetic process | 7 | 0.610288 | 1.58E-05 |
| Purine ribonucleoside monophosphate biosynthetic process | 7 | 0.610288 | 2.80E-05 |
| Mitotic sister chromatid segregation | 9 | 0.784656 | 3.03E-05 |
| Telomere maintenance via recombination | 10 | 0.87184 | 3.08E-05 |
| Response to drug | 35 | 3.051439 | 3.63E-05 |
| Response to unfolded protein | 11 | 0.959024 | 5.44E-05 |
| DNA repair | 29 | 2.528335 | 5.73E-05 |
| DNA synthesis involved in DNA repair | 10 | 0.87184 | 6.71E-05 |
| DNA strand elongation involved in DNA replication | 7 | 0.610288 | 7.45E-05 |
| Pyrimidine nucleoside biosynthetic process | 5 | 0.43592 | 1.10E-04 |
| Spindle organization | 7 | 0.610288 | 1.14E-04 |
| Organ regeneration | 11 | 0.959024 | 1.50E-04 |
| Cellular response to hypoxia | 16 | 1.394943 | 1.62E-04 |
| rRNA transcription | 6 | 0.523104 | 2.46E-04 |
| Sprouting angiogenesis | 8 | 0.697472 | 2.46E-04 |
| Ribosomal large subunit biogenesis | 8 | 0.697472 | 2.46E-04 |
| Strand displacement | 8 | 0.697472 | 3.21E-04 |
| Canonical glycolysis | 8 | 0.697472 | 3.21E-04 |
| Response to hypoxia | 22 | 1.918047 | 3.34E-04 |
| G2/M transition of mitotic cell cycle | 19 | 1.656495 | 3.56E-04 |
| Positive regulation of gene expression, epigenetic | 12 | 1.046207 | 3.87E-04 |
| Response to starvation | 9 | 0.784656 | 4.10E-04 |
| DNA replication checkpoint | 5 | 0.43592 | 4.72E-04 |

For Peer Review

| | | | |
|---|---|---|---|
| Double-strand break repair via homologous recombination | 13 | 1.133391 | 5.05E-04 |
| Mitotic metaphase plate congression | 9 | 0.784656 | 6.12E-04 |
| Positive regulation of establishment of protein localization to telomere | 5 | 0.43592 | 8.14E-04 |
| Positive regulation of telomerase RNA localization to Cajal body | 6 | 0.523104 | 8.16E-04 |
| Maturation of LSU-rRNA | 6 | 0.523104 | 8.16E-04 |
| Mitotic spindle organization | 8 | 0.697472 | 8.26E-04 |
| Regulation of signal transduction by p53 class mediator | 17 | 1.482127 | 9.05E-04 |
| Maturation of SSU-rRNA from tricistronic rRNA transcript (SSU-rRNA, 5.8S rRNA, LSU-rRNA) | 8 | 0.697472 | 0.001244 |
| Positive regulation of telomere maintenance via telomerase | 8 | 0.697472 | 0.001244 |
| Chaperone mediated protein folding requiring cofactor | 5 | 0.43592 | 0.0013 |
| Purine nucleobase biosynthetic process | 4 | 0.348736 | 0.001392 |
| Cellular response to DNA damage stimulus | 23 | 2.005231 | 0.001706 |
| CENP-A containing nucleosome assembly | 9 | 0.784656 | 0.001733 |
| DNA duplex unwinding | 9 | 0.784656 | 0.002021 |
| Double-strand break repair | 11 | 0.959024 | 0.002456 |
| Toxin transport | 8 | 0.697472 | 0.002563 |
| Ribosome biogenesis | 8 | 0.697472 | 0.002563 |
| Cell cycle | 23 | 2.005231 | 0.0029 |
| Spliceosomal snRNP assembly | 7 | 0.610288 | 0.003093 |
| Cytokinesis | 9 | 0.784656 | 0.003567 |
| Mitotic cytokinesis | 7 | 0.610288 | 0.003727 |
| Protein sumoylation | 15 | 1.307759 | 0.003749 |
| Protein folding in endoplasmic reticulum | 5 | 0.43592 | 0.003892 |
| Regulation of cyclin-dependent protein serine/threonine kinase activity | 8 | 0.697472 | 0.00411 |
| Cellular response to gamma radiation | 6 | 0.523104 | 0.004234 |
| Positive regulation of cell migration | 20 | 1.743679 | 0.004437 |
| Response to testosterone | 7 | 0.610288 | 0.004452 |
| DNA damage checkpoint | 7 | 0.610288 | 0.004452 |
| Positive regulation of mitotic cell cycle spindle assembly checkpoint | 4 | 0.348736 | 0.004493 |
| Maturation of SSU-rRNA | 5 | 0.43592 | 0.005221 |
| Mitotic cell cycle checkpoint | 7 | 0.610288 | 0.006207 |
| Lactation | 8 | 0.697472 | 0.006279 |
| Protein heterotetramerization | 8 | 0.697472 | 0.006279 |
| Regulation of chromosome segregation | 4 | 0.348736 | 0.006905 |
| Positive regulation of protein localization to Cajal body | 4 | 0.348736 | 0.006905 |

For Peer Review

| | | | |
|---|---|---|---|
| Mitotic spindle midzone assembly | 4 | 0.348736 | 0.006905 |
| Endonucleolytic cleavage in ITS1 to separate SSU-rRNA from 5.8S rRNA and LSU-rRNA from tricistronic rRNA transcript (SSU-rRNA, 5.8S rRNA, LSU-rRNA) | 4 | 0.348736 | 0.006905 |
| Negative regulation of B cell apoptotic process | 4 | 0.348736 | 0.006905 |
| Regulation of dendrite development | 4 | 0.348736 | 0.006905 |
| Cellular response to UV | 8 | 0.697472 | 0.008136 |
| Mitotic nuclear envelope disassembly | 8 | 0.697472 | 0.008136 |
| Histone H3-K9 dimethylation | 3 | 0.261552 | 0.008212 |
| De novo' UMP biosynthetic process | 3 | 0.261552 | 0.008212 |
| Epithelial to mesenchymal transition | 7 | 0.610288 | 0.008417 |
| Ribosomal small subunit biogenesis | 5 | 0.43592 | 0.008719 |
| Cerebral cortex development | 9 | 0.784656 | 0.009245 |
| Base-excision repair | 7 | 0.610288 | 0.009711 |
| Cholesterol metabolic process | 10 | 0.87184 | 0.00975 |
| Attachment of spindle microtubules to kinetochore | 4 | 0.348736 | 0.009951 |
| Maturation of LSU-rRNA from tricistronic rRNA transcript (SSU-rRNA, 5.8S rRNA, LSU-rRNA) | 4 | 0.348736 | 0.009951 |
| ATF6-mediated unfolded protein response | 4 | 0.348736 | 0.009951 |
| Protein maturation by protein folding | 4 | 0.348736 | 0.009951 |
| Nucleosome assembly | 14 | 1.220575 | 0.010831 |
| Negative regulation of transcription, DNA-templated | 40 | 3.487358 | 0.010879 |
| DNA biosynthetic process | 6 | 0.523104 | 0.010982 |
| DNA recombination | 11 | 0.959024 | 0.01261 |
| Positive regulation of vascular endothelial growth factor production | 6 | 0.523104 | 0.0129 |
| Microtubule polymerization | 4 | 0.348736 | 0.013658 |
| Microtubule depolymerization | 4 | 0.348736 | 0.013658 |
| Interstrand cross-link repair | 8 | 0.697472 | 0.014507 |
| Peptidyl-arginine N-methylation | 3 | 0.261552 | 0.015843 |
| scaRNA localization to Cajal body | 3 | 0.261552 | 0.015843 |
| Kidney development | 11 | 0.959024 | 0.015931 |
| Negative regulation of DNA replication | 5 | 0.43592 | 0.016355 |
| Nucleoside metabolic process | 5 | 0.43592 | 0.016355 |
| DNA damage response, signal transduction by p53 class mediator resulting in cell cycle arrest | 9 | 0.784656 | 0.016662 |
| Positive regulation of telomerase activity | 6 | 0.523104 | 0.017387 |
| Double-strand break repair via nonhomologous end joining | 9 | 0.784656 | 0.018223 |
| Mitotic spindle assembly checkpoint | 5 | 0.43592 | 0.019601 |
| G2 DNA damage checkpoint | 5 | 0.43592 | 0.019601 |
| Glutamine metabolic process | 5 | 0.43592 | 0.019601 |

For Peer Review

| | | | |
|---|---|---|---|
| Intrinsic apoptotic signaling pathway in response to DNA damage by p53 class mediator | 6 | 0.523104 | 0.022801 |
| Negative regulation of transcription from RNA polymerase II promoter | 52 | 4.533566 | 0.023118 |
| Metaphase plate congression | 4 | 0.348736 | 0.023124 |
| PERK-mediated unfolded protein response | 4 | 0.348736 | 0.023124 |
| Positive regulation of fibroblast proliferation | 8 | 0.697472 | 0.023821 |
| Histone H3-K9 trimethylation | 3 | 0.261552 | 0.025478 |
| AMP biosynthetic process | 3 | 0.261552 | 0.025478 |
| Ribonucleoside monophosphate biosynthetic process | 3 | 0.261552 | 0.025478 |
| Ddouble-strand break repair via break-induced replication | 3 | 0.261552 | 0.025478 |
| Cellular response to xenobiotic stimulus | 3 | 0.261552 | 0.025478 |
| Regulation of striated muscle tissue development | 3 | 0.261552 | 0.025478 |
| Response to inorganic substance | 3 | 0.261552 | 0.025478 |
| Response to activity | 7 | 0.610288 | 0.025493 |
| DNA replication-dependent nucleosome assembly | 6 | 0.523104 | 0.025874 |
| Positive regulation of neutrophil chemotaxis | 5 | 0.43592 | 0.027211 |
| Positive regulation of protein complex assembly | 5 | 0.43592 | 0.027211 |
| Chaperone-mediated protein complex assembly | 4 | 0.348736 | 0.028894 |
| Protein stabilization | 14 | 1.220575 | 0.029622 |
| Protein folding | 17 | 1.482127 | 0.031226 |
| NLS-bearing protein import into nucleus | 5 | 0.43592 | 0.031591 |
| Negative regulation of myoblast differentiation | 5 | 0.43592 | 0.031591 |
| Regulation of ubiquitin-protein ligase activity involved in mitotic cell cycle | 5 | 0.43592 | 0.031591 |
| Transmembrane receptor protein tyrosine kinase signaling pathway | 11 | 0.959024 | 0.031708 |
| Epithelial cell differentiation | 9 | 0.784656 | 0.032184 |
| Glycolytic process | 6 | 0.523104 | 0.032782 |
| Negative regulation of smooth muscle cell migration | 4 | 0.348736 | 0.035351 |
| Oxidation-reduction process | 43 | 3.74891 | 0.036266 |
| Meiotic nuclear division | 5 | 0.43592 | 0.036359 |
| Regulation of mitotic nuclear division | 5 | 0.43592 | 0.036359 |
| Cellular response to interleukin-4 | 5 | 0.43592 | 0.036359 |
| Binding of sperm to zona pellucida | 6 | 0.523104 | 0.036627 |
| Tetrahydrofolate biosynthetic process | 3 | 0.261552 | 0.03688 |
| DNA replication, synthesis of RNA primer | 3 | 0.261552 | 0.03688 |
| Endonucleolytic cleavage in 5'-ETS of tricistronic rRNA transcript (SSU-rRNA, 5.8S rRNA, LSU-rRNA) | 3 | 0.261552 | 0.03688 |
| Positive regulation of exit from mitosis | 3 | 0.261552 | 0.03688 |
| De novo' pyrimidine nucleobase biosynthetic process | 3 | 0.261552 | 0.03688 |

For Peer Review

| | | | |
|---|---|---|---|
| Histone H4-R3 methylation | 3 | 0.261552 | 0.03688 |
| Response to cold | 6 | 0.523104 | 0.040738 |
| Mitotic spindle assembly | 6 | 0.523104 | 0.040738 |
| Microtubule bundle formation | 5 | 0.43592 | 0.041519 |
| Response to cadmium ion | 5 | 0.43592 | 0.041519 |
| Positive regulation of phosphorylation | 5 | 0.43592 | 0.041519 |
| Nucleobase-containing small molecule interconversion | 5 | 0.43592 | 0.041519 |
| Cell migration | 16 | 1.394943 | 0.041694 |
| Protein refolding | 4 | 0.348736 | 0.042483 |
| Response to copper ion | 4 | 0.348736 | 0.042483 |
| Positive regulation of angiogenesis | 12 | 1.046207 | 0.042934 |
| Response to ionizing radiation | 7 | 0.610288 | 0.044815 |
| Nucleobase-containing compound metabolic process | 7 | 0.610288 | 0.044815 |
| Adherens junction organization | 6 | 0.523104 | 0.045117 |
| Chromatin silencing at rDNA | 6 | 0.523104 | 0.045117 |
| Response to endoplasmic reticulum stress | 9 | 0.784656 | 0.045757 |
| Regulation of cellular response to heat | 9 | 0.784656 | 0.045757 |
| tRNA methylation | 5 | 0.43592 | 0.047072 |
| Positive regulation of protein tyrosine kinase activity | 5 | 0.43592 | 0.047072 |
| DNA replication-independent nucleosome assembly | 5 | 0.43592 | 0.047072 |
| Box C/D snoRNP assembly | 3 | 0.261552 | 0.049836 |
| Axon ensheathment | 3 | 0.261552 | 0.049836 |
| Strand invasion | 3 | 0.261552 | 0.049836 |

For Peer Review

Table S4. List of gene from microarray analysis data of HSC-4 cells cultured in 2D culture and suspension culture.

| Gene Symbol | EntrezGeneID | Ratio 2D culture vs suspension culture |
|---|---|---|
| AREG | 374 | 0.17 |
| AURKB | 9212 | 0.04 |
| CCND1 | 595 | 0.52 |
| CDK6 | 1021 | 0.43 |
| E2F1 | 1869 | 0.05 |
| FOXM1 | 2305 | 0.10 |
| KIF23 | 9493 | 0.08 |
| MCM7 | 4176 | 0.07 |
| PIEZO1 | 9780 | 0.94 |
| PIEZO2 | 63895 | NULL |

For Peer Review

# Hasegawa *et al*., Figure S1

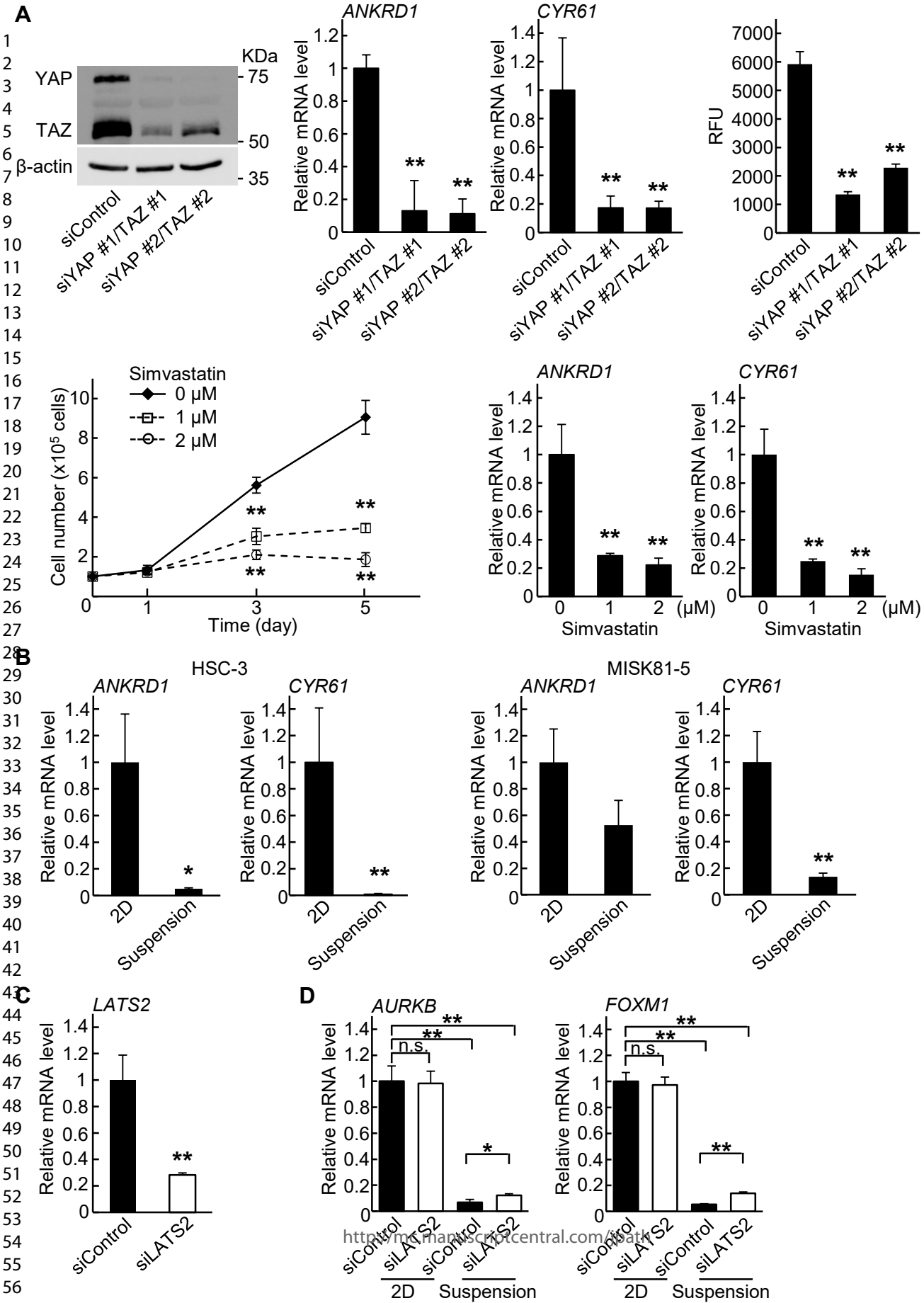


http://mc.manuscriptcentral.com/jpath

**Supplementary Figure 1.** The effect of YAP/TAZ signaling on OSCC cells.
(A) HSC-4 cells were transfected with control or two different YAP/TAZ siRNAs for 48 h. Cell lysates were probed with anti-YAP/TAZ and anti-β-actin antibodies (upper left panel). Molecular weight size was noted referring to molecular weight marker. *ANKRD1* and *CYR61* mRNA levels in the cells were also measured by quantitative RT-PCR. Relative levels of *ANKRD1* and *CYR61* mRNA expression were normalized to *GAPDH* and expressed as fold-changes compared with levels in control siRNA transfected cells (upper middle panels). The cells were cultured in the presence of 5% FBS for 48 h, and relative cell numbers were quantified using the CyQUANT cell proliferation assay (upper right panel). RFU: relative fluorescence units. HSC-4 cells were cultured without or with 1 and 2 μM Simvastatin. The cells were cultured in the presence of 5% FBS for the indicated numbers of days, and cell numbers were counted (lower left panel). *ANKRD1* and *CYR61* mRNA levels in the cells were also measured by quantitative RT-PCR. Relative levels of *ANKRD1* and *CYR61* mRNA expression were normalized to *GAPDH* and expressed as fold-changes compared with levels in control siRNA transfected cells (lower right panel). (B) *ANKRD1* and *CYR61* mRNA levels in HSC-3 and MISK81-5 cells cultured in 2D or suspension culture for 24 h were measured by quantitative RT-PCR. Relative levels of *ANKRD1* and *CYR61* mRNA expression were normalized to *GAPDH* and expressed as fold-changes compared with expression in 2D cells. (C) HSC-4 cells were transfected with control or LATS2 siRNA for 48 h, and *LATS2* mRNA levels were measured by quantitative RT-PCR. Relative *LATS2* mRNA levels were normalized by *GAPDH* and expressed as fold-changes compared with levels in control siRNA transfected cells. (D) HSC-4 cells were transfected with control or LATS2 siRNA for 48 h, and then cells were cultured in 2D or suspension culture for 24 h. *AURKB* and *FOXM1* mRNA levels were measured by quantitative RT-PCR. Relative levels of *AURKB* and *FOXM1* mRNA expression were normalized to *GAPDH* and expressed as fold-changes compared with levels in 2D control cells. Results are shown as means ± s.d. of three independent experiments. **P*<0.05, ***P*<0.01. n.s.: not significant.

# Hasegawa *et al.*, Figure S2

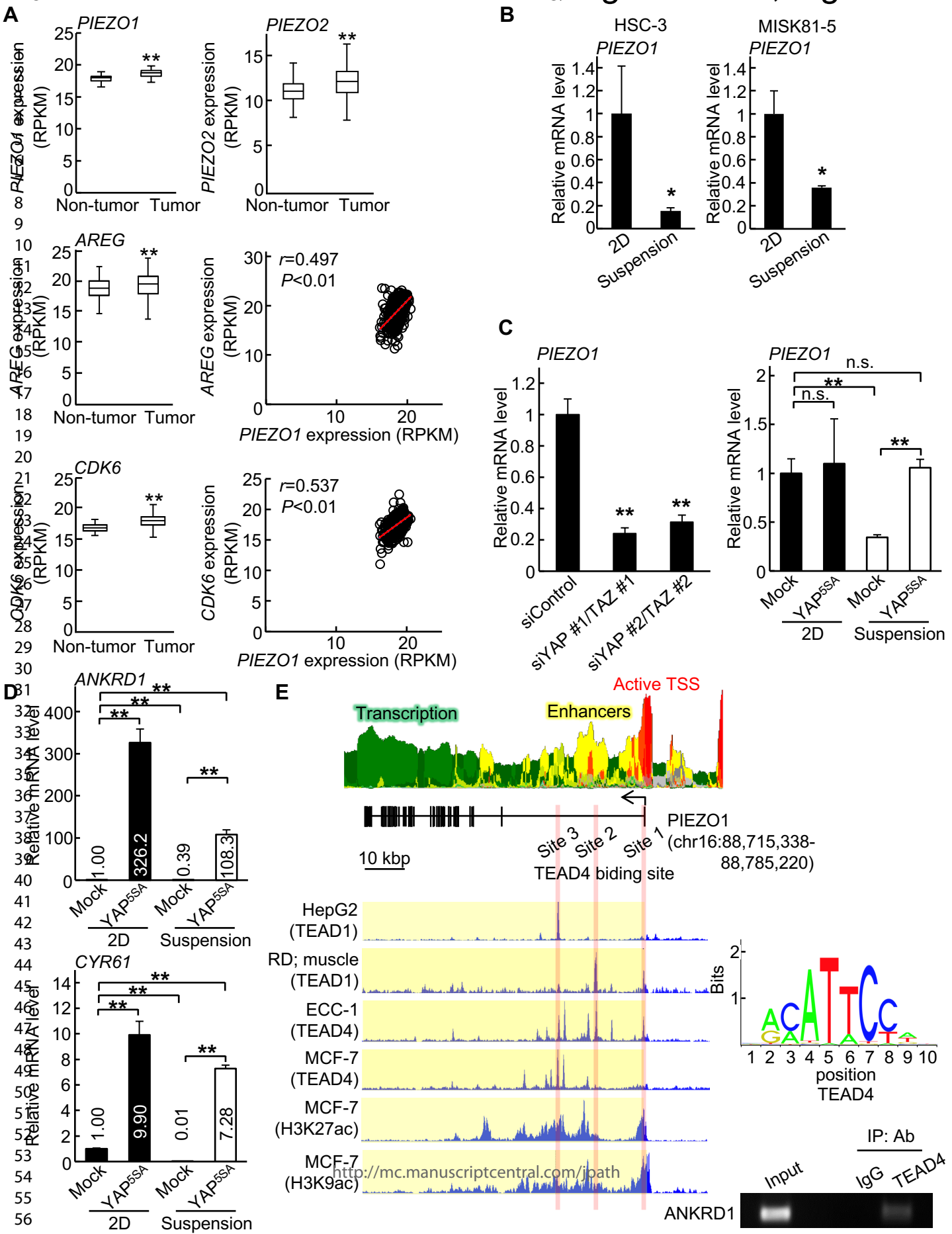


http://mc.manuscriptcentral.com/joath

**Supplementary Figure 2.** YAP signaling regulates PIEZO1 expression in OSCC cells.
(A) The expression of *PIEZO1, PIEZO2, AREG* or *CDK6* in 518 tumor lesions and 44 non-tumor regions in head and neck region was evaluated using TCGA dataset. Correlation between *PIEZO1* and *AREG* or *CDK6* mRNA was examined in the tumor lesion. RPKM, reads per kilobase per million reads. Spearman's rank rho was used to calculate the "r" correlation coefficient. (B) *PIEZO1* mRNA levels in HSC-3 and MISK81-5 cells cultured in 2D or suspension culture for 24 h were measured by quantitative RT-PCR. Relative levels of *PIEZO1* mRNA expression were normalized to *GAPDH* and expressed as fold-changes compared with expression in 2D cells. (C) HSC-3 cells were transfected with control or two different YAP/TAZ siRNAs for 48 h, and then cells were cultured in 2D culture for 3 h. *PIEZO1* mRNA levels were measured by quantitative RT-PCR. Relative *PIEZO1* mRNA levels were normalized by *GAPDH* and expressed as fold-changes compared with levels in control siRNA transfected cells (left panel). HSC-3 cells expressing mock or $YAP^{5SA}$ were cultured in 2D or suspension culture for 24 h and *PIEZO1* mRNA levels were measured by quantitative RT-PCR. Relative levels of *PIEZO1* mRNA expression were normalized to *GAPDH* and expressed as fold-changes compared with expression in 2D control cells (right panel). (D) HSC-4 cells expressing mock or $YAP^{5SA}$ were cultured in 2D or suspension culture for 24 h, and *ANKRD1* and *CYR61* mRNA levels were measured by quantitative RT-PCR. Relative levels of *ANKRD1* and *CYR61* mRNA expression were normalized to *GAPDH* and expressed as fold-changes compared with expression in 2D control cells. (E) Genomic views of TEAD1, TEAD4, H3K27ac and H3K9ac ChIP enrichment at human *PIEZO1* gene obtained from Cistrome Data Browser database. The *PIEZO1* gene enhancer region contains three predicted TEAD4-binding sites. Chromatin from HSC-4 cells expressing mock was immunoprecipitated with anti-control IgG or anti-TEAD4 antibody, and the precipitates were analyzed by PCR for TEAD4 binding site of the *ANKRD1* gene promoter. Results are shown as means ± s.d. of three independent experiments. $*P<0.05$, $**P<0.01$. n.s.: not significant.

# Hasegawa *et al.*, Figure S3

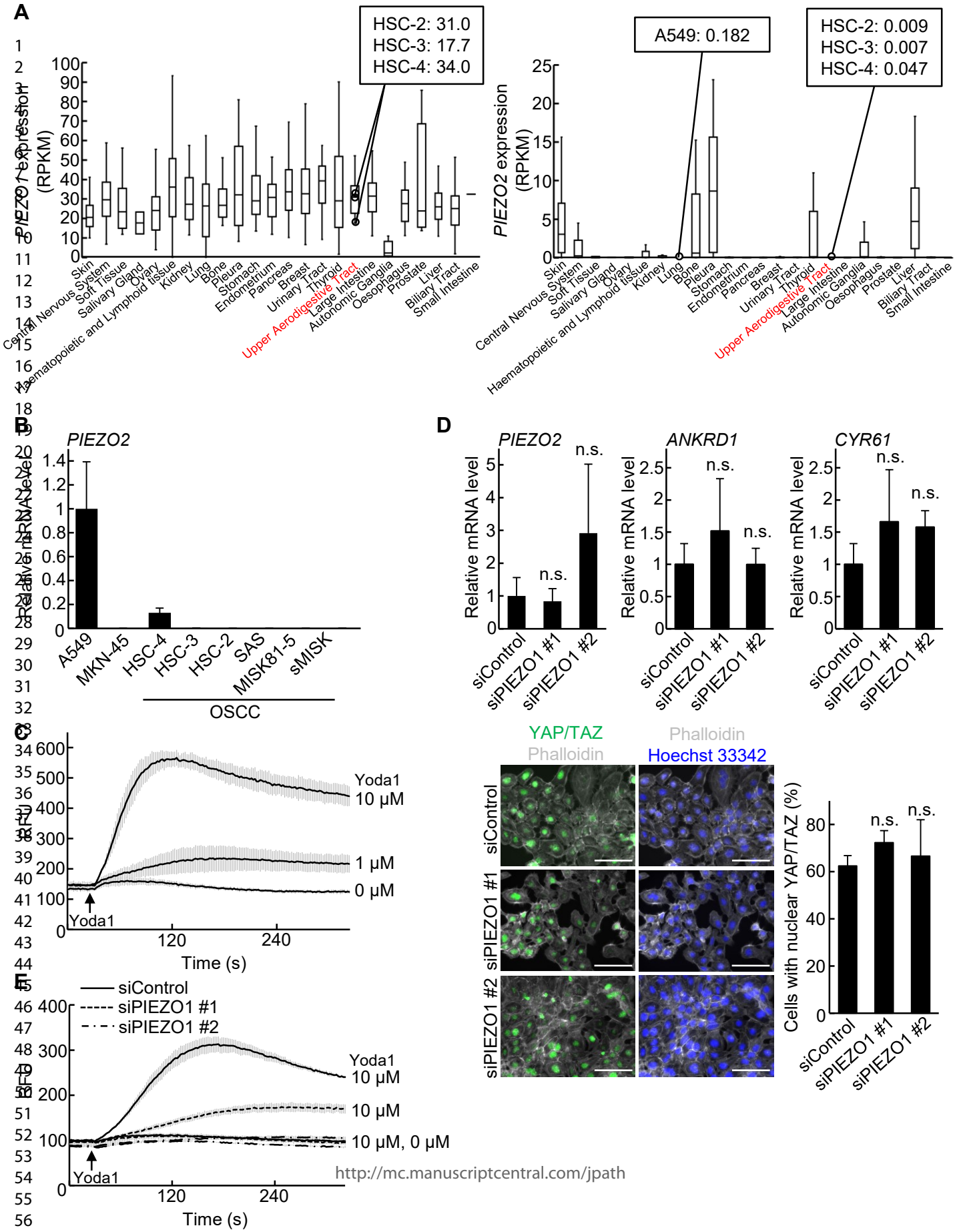

**Supplementary Figure 3.** The effect of PIEZO1 on YAP/TAZ signaling.
(A) The expression of *PIEZO1* and *PIEZO2* in cell lines was evaluated using Cancer Cell Line Encyclopedia dataset. (B) *PIEZO2* mRNA levels were measured in OSCC cell lines (HSC-4, HSC-3, HSC-2, SAS, MISK81-5 and sMISK cells), A549 and MKN-45 cells by quantitative RT-PCR. Relative levels of *PIEZO2* mRNA expression were normalized to *GAPDH* and expressed as fold-changes compared with expression in control A549 cells. (C) HSC-4 cells were pre-loaded with Fluo-4-AM and were exposed without or with 1 and 10 μM Yoda1. Then, intracellular $Ca^{2+}$ influx was measured. RFU: relative fluorescence units. (D) HSC-4 cells were transfected with control or two different PIEZO1 siRNAs for 48 h, and *PIEZO2*, *ANKRD1* and *CYR61* mRNA levels were measured by quantitative RT-PCR. Relative *PIEZO2*, *ANKRD1* and *CYR61* mRNA levels were normalized by *GAPDH* and expressed as fold-changes compared with levels in control siRNA transfected cells (upper panels). HSC-4 cells were transfected with control or two different PIEZO1 siRNAs for 48 h, and the cells were stained with anti-YAP/TAZ antibody, phalloidin and Hoechst 33342. Cells with nuclear YAP/TAZ are expressed as the percentage of YAP/TAZ-positively stained cells compared with total Hoechst 33342-stained cells ($n$ = 1516) (lower panels). (E) HSC-4 cells transfected with control or two different PIEZO1 siRNAs were pre-loaded with Fluo-4-AM and were exposed without or with 10 μM Yoda1. Then, intracellular $Ca^{2+}$ influx was measured. RFU: relative fluorescence units. Results are shown as means ± s.d. of three independent experiments. Scale bars, 100 μm. n.s.: not significant.

# Hasegawa *et al.*, Figure S4

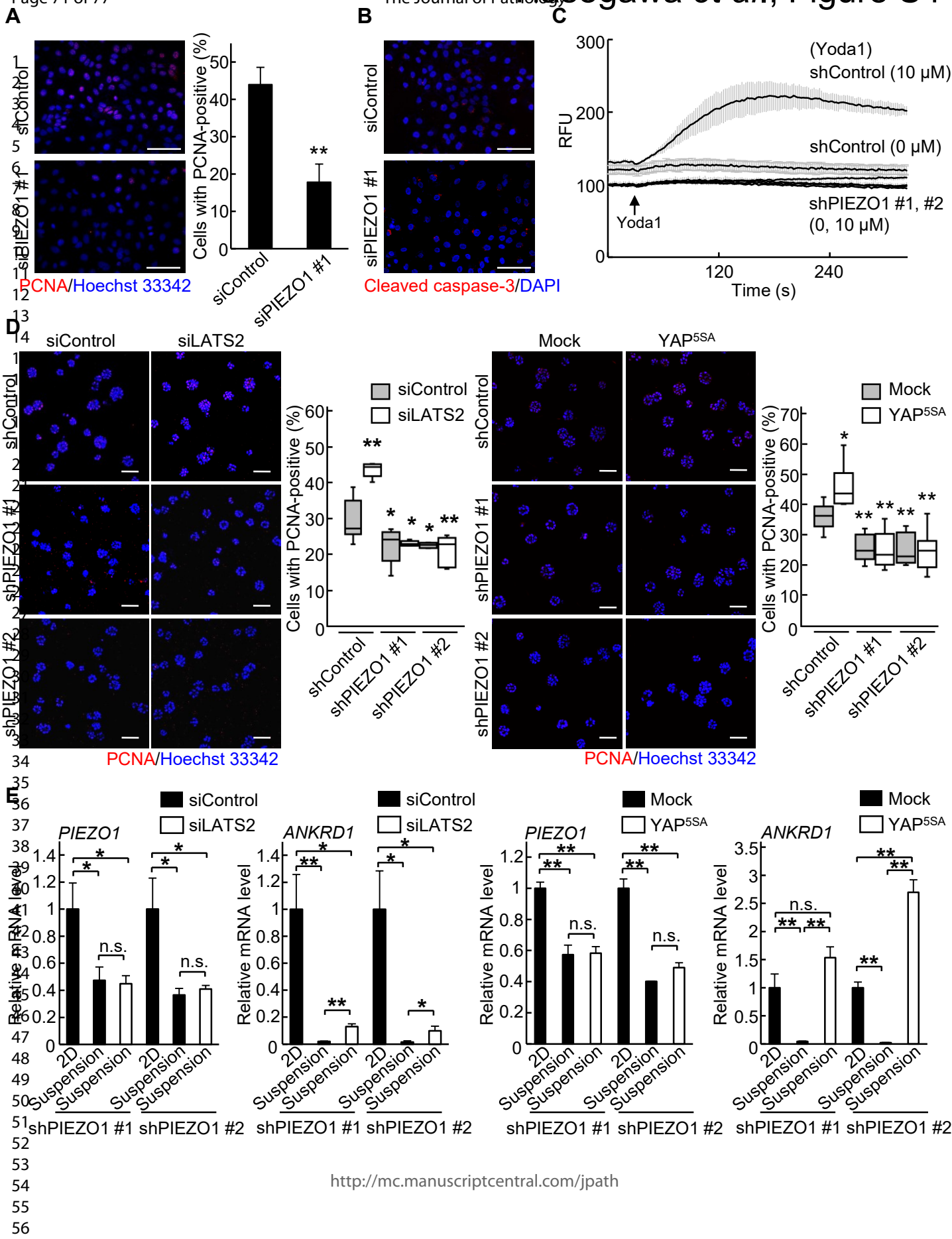

**Supplementary Figure 4.** PIEZO1 regulates cell proliferation of OSCC cells.
(A) HSC-4 cells were transfected with control or PIEZO1 #1 siRNA for 48 h. The cells were stained with anti-PCNA antibody and Hoechst 33342, and then PCNA-positive cells and Hoechst 33342-stained cells were counted, respectively. Results are expressed as the percentage of PCNA-positive cells compared with total Hoechst 33342-stained cells. (B) HSC-4 cells were transfected with control or PIEZO1 #1 siRNA for 48 h. The cells were stained with anti-cleaved caspase-3 antibody and DAPI. (C) HSC-4 cells expressing control or PIEZO1 #1 and #2 shRNAs were pre-loaded with Fluo-4-AM and were exposed without or with 10 μM Yoda1. Then, intracellular $Ca^{2+}$ influx was measured. RFU: relative fluorescence units. (D) HSC-4 cells expressing control or PIEZO1 #1 and #2 shRNAs were transfected with control or LATS2 siRNA for 48 h (left panels) or with mock or $YAP^{5SA}$ expression (right panels), and then cells were cultured for 4 days in the 3D Matrigel. The cells were stained with anti-PCNA antibody and Hoechst 33342, and then PCNA-positive cells and Hoechst 33342-stained cells were counted, respectively. Results are expressed as the percentage of PCNA-positively stained cells compared with total Hoechst 33342-stained cells ($n$ = 14,242). (E) HSC-4 cells expressing PIEZO1 #1 and #2 shRNAs were transfected with control or LATS2 siRNA for 48 h (left panels) or with mock or $YAP^{5SA}$ expression (right panels), and then cells were cultured in 2D or suspension culture for 24 h. *PIEZO1* or *ANKRD1* mRNA levels were measured by quantitative RT-PCR. Relative *PIEZO1* or *ANKRD1* mRNA levels were normalized by *GAPDH* and expressed as fold-changes compared with levels in 2D control cells. Results are shown as means ± s.d. of three independent experiments. *$P$<0.05, **$P$<0.01. Scale bars, 100 μm. n.s.: not significant.

Hasegawa *et al*., Figure S5

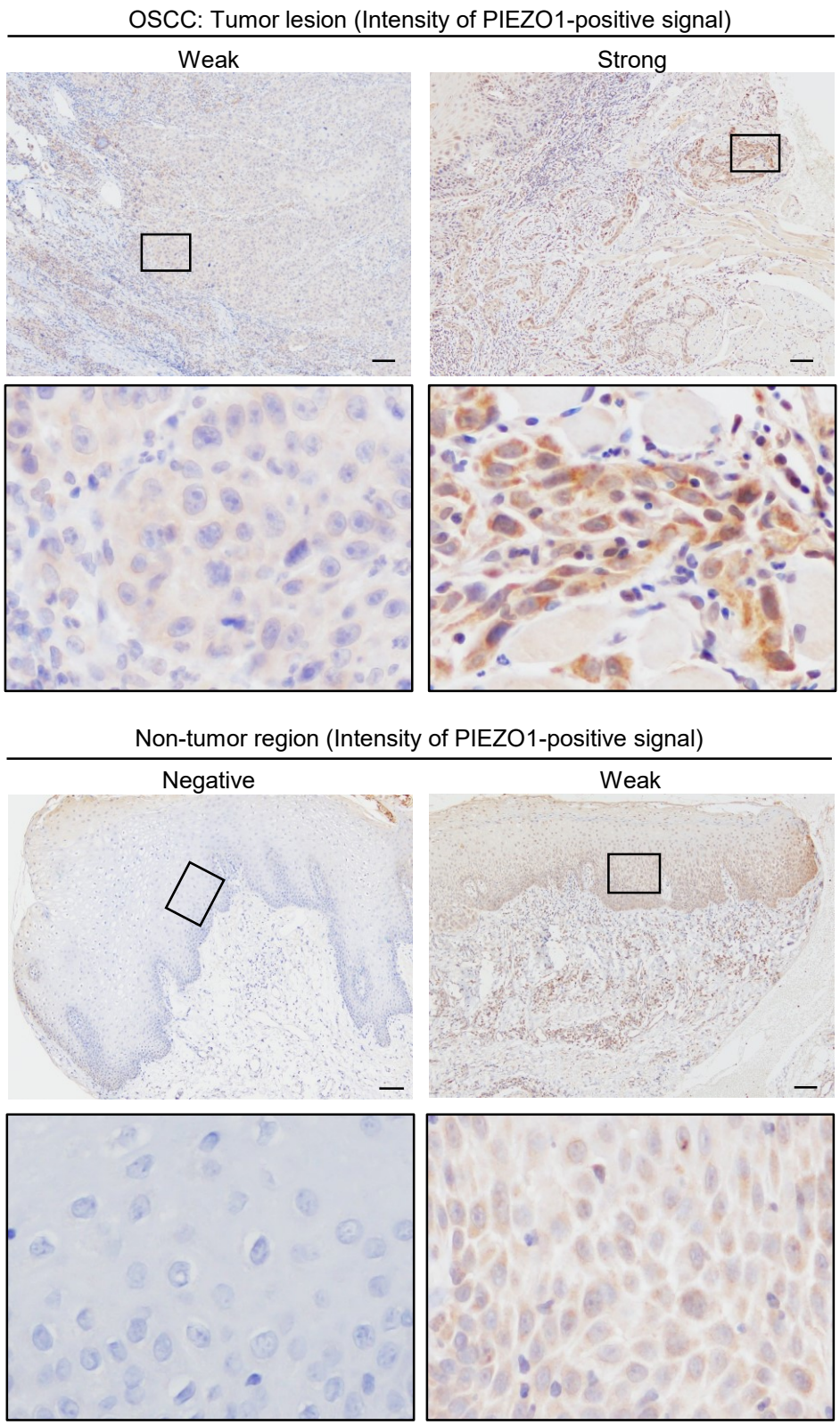


**Supplementary Figure 5.** PIEZO1 is expressed in human oral squamous cell carcinoma tissues. Oral squamous cell carcinoma tissues ($n$ = 45) were stained with anti-PIEZO1 antibody and hematoxylin. PIEZO1-positive signal intensity was classified as follows: negative; weak; strong. Boxes show enlarged images. Scale bars, 100 μm.

http://mc.manuscriptcentral.com/jpath

# Hasegawa *et al*., Figure S6

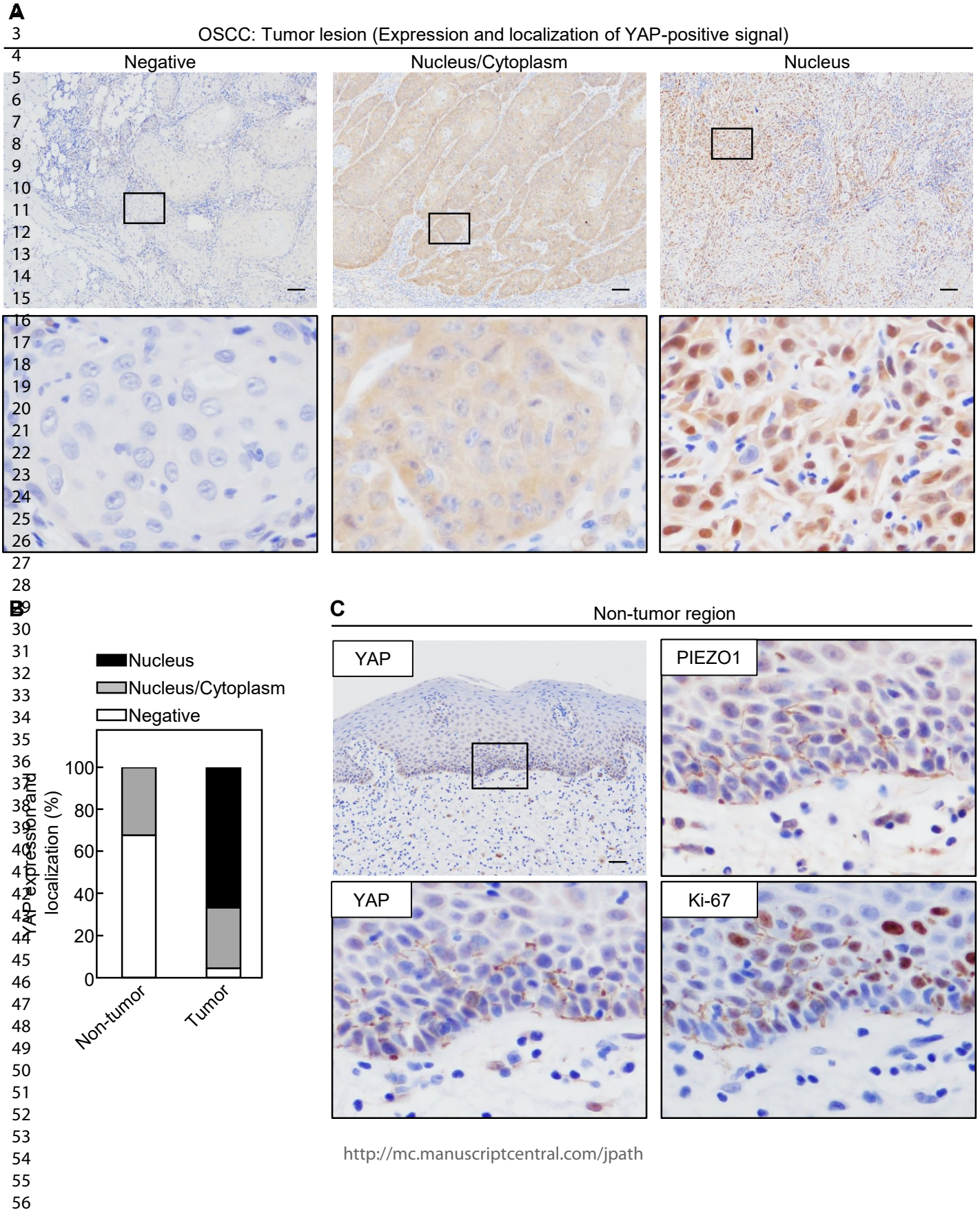

**Supplementary Figure 6.** YAP is expressed in human oral squamous cell carcinoma tissues. (A) Oral squamous cell carcinoma tissues ($n$ = 45) were stained with anti-YAP antibody and hematoxylin. YAP expression and localization were classified as follows: negative; nucleus/cytoplasm; nucleus. Boxes show enlarged images. (B) Percentages of three groups based on the YAP expression and localization in the tumor lesions and the non-tumor regions are shown in the panel. (C) Oral squamous cell carcinoma tissues ($n$ = 45) were stained with anti-YAP, anti-PIEZO1 and anti-Ki-67 antibodies, and hematoxylin. Box shows enlarged images. Scale bars, 50 μm.

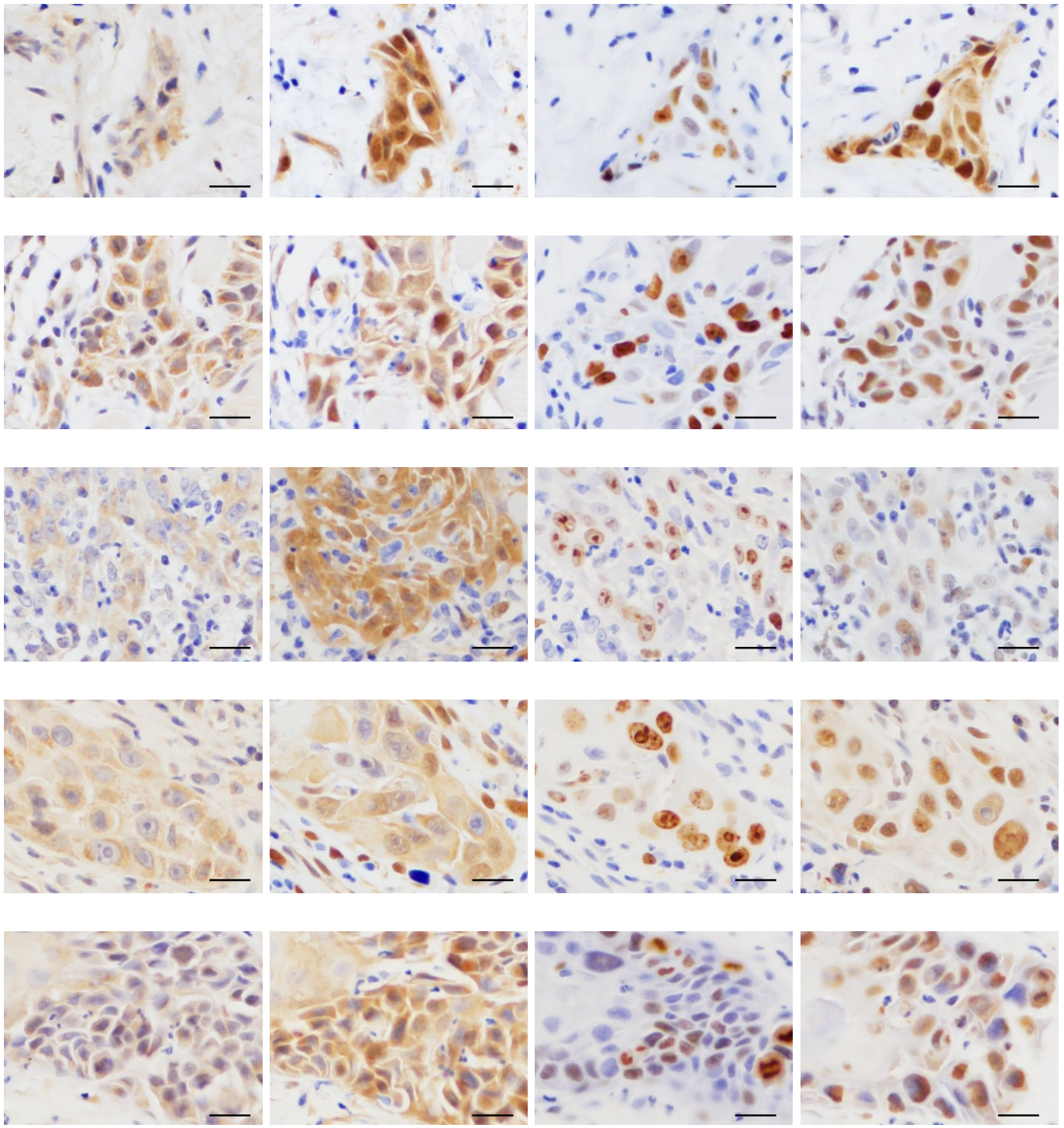


**Supplementary Figure 7.** Co-expression of PIEZO1, YAP, Ki-67 and PCNA in human oral squamous cell carcinoma tissues.

Oral squamous cell carcinoma tissues ($n$ = 45) were stained with anti-PIEZO1, anti- YAP, anti-Ki-67 and anti-PCNA antibodies, and hematoxylin. Representative data (n = 5) are shown. Scale bars, 20 μm.

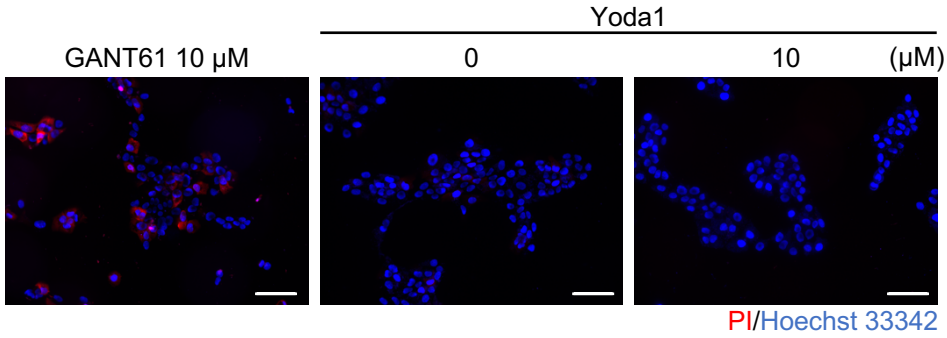


**Response to Reviewer #1 Figure 1.** The vitality of the cells treated with Yoda1. HSC-4 cells were treated with 10 μM GANT61 in the absence of FBS for 24 h, or without or with 10 μM Yoda1 in the presence of 10% FBS for 5 min (see Figure 3B). The cells were stained with Propidium Iodide (PI) and Hoechst 33342. GANT61, a GLI-1 and GLI-2 inhibitor, was treated as a positive control [1]. Scale bars, 100 μm.

[1] Mikami Y, Fujii S, Nagata K, et al. GLI-mediated Keratin 17 expression promotes tumor cell growth through the anti-apoptotic function in oral squamous cell carcinomas. *J Cancer Res Clin Oncol* 2017; **143**: 1381-1393.